KTH Engineering Sciences

Design of Multifunctional Body Panels in Automotive Applications

Reducing the Ecological and Economical footprint of the vehicle industry

CHRISTOPHER J. CAMERON

Licentiate Thesis
Stockholm, Sweden 2009

TRITA-AVE2009-30
ISSN 1651-7660
ISBN 978-91-7415-362-0

KTH School of Engineering Sciences
SE-100 44 Stockholm
SWEDEN

Akademisk avhandling som med tillstånd av Kungl Tekniska högskolan framlägges till offentlig granskning för avläggande av teknologie licentiatsexamen i lättkonstruktioner Måndagen den 8 juni 2009, klockan 13.15 i sal D3, Kungliga Tekniska Högskolan, Lindstedtsvägen 5, Stockholm.

Tryck: Universitetsservice US-AB

Abstract

Over the past century, the automobile has become an integral part of modern industrialized society. Consumer demands, regulatory legislation, and the corporate need to generate a profit, have been the most influential factors in driving forward the evolution of the automobile. As the comfort, safety, and reliability of the automobile have increased, so has its complexity, and most definitely its mass.

The work within this thesis addresses the twofold problem of economy and ecology with respect to sustainable development of automobiles. Specifically, the conflicting problems of reducing weight, and maintaining or improving noise, vibration, and harshness behaviour are addressed. Potential solutions to these problems must also be executable at the same, or preferably lower production costs. The hypothesis is that by replacing acoustic treatments, aesthetic details, and complex systems of structural components both on the interior and exterior of the vehicle with a single multi-functional body panel, functionality can be retained at a reduced mass (i.e. reduced consumption of raw materials) and reduced fiscal cost.

A case study is performed focusing on the roof structure of a production vehicle. Full vehicle and component level acoustic testing is performed to acquire acoustic functional requirements. Vibro-mechanical testing at the component level is performed to acquire structural functional requirements complimentary to those in the vehicles design specifications. Finite element modelling and analysis is employed to create a model representative of the as-tested component and evaluate its acoustic and mechanical behaviour numerically. Results of numerical simulations are compared with the measured results for both acoustic and mechanical response in order to verify the model and firmly establish a set of acoustic and mechanical constraints for future work.

A new, multi-layered, multi-functional sandwich panel concept is proposed which replaces the outer sheet metal, damping treatments, transverse beams, and interior trim of the existing structure. The new panel is weight optimized to a set of structural constraints and its acoustic properties are evaluated. Results show a significant reduction in mass compared to the existing system with no degradation of the acoustic environment.

A discussion of the results is presented, as is a suggestion for future research.

Acknowledgements

The work presented in this thesis has been carried out within the centre for ECO^2 Vehicle Design at the Department of Aeronautical and Vehicle Engineering, KTH.

Funding is provided via Vinnova and industrial partners Saab Automobile AB, Bombardier Transportation, and A2 Acoustics. The financial support of all parties is gratefully acknowledged.

I would like to thank Dr. Per Wennhage and Professor Peter Göransson, firstly for giving me a chance at being a researcher, and secondly for all their help and advice thus far.

This project would of course not have been possible without the help of Saab Automobile AB and more specifically, Mr. Sven Rahmqvist; thank you for your assistance an input. I am also grateful for the assistance of Eva-Lotta Saloniemi Modin for helping with nastran problems both large and small.

To Associate Professor Leping Feng for his assistance in performing measurements both at Saab and MWL and in his assistance in post processing some of the results, I extend my gratitude.

I cannot forget thank Professor Zenkert, the other senior members, my colleagues and our lab engineers within the division of lightweight structures. Everyone there has at some point helped me along the way. I have enjoyed working with all of you and look forward to continuing to do so. To Mr. Kaufmann, thanks for, among other things, interesting lunch box discussions and your knowledge of fine cheese. To Mr. Stig, a special thanks for balancing out the office. What would the world be like without telemark skis and Apple® computers?

To my family, thank you for lending your support from all the way across the pond.

Last, but not least, to my biggest source of love, strength, and inspiration; Camilla. Without you I never would have made it this far. Thank you.

Stockholm, May 2009

As this thesis may be read outside of Sweden an explanation of the Swedish Licentiate degree may be necessary. An intermediate academic degree called Licentiate of Technology can be obtained half-way between an MSc and a PhD. While less formal than a Doctoral Dissertation, examination for the degree includes writing a thesis and a public thesis defence.

Dissertation

This licentiate thesis is based on an introduction to the area of research and the following appended papers:

Paper A

Christopher J. Cameron, Per Wennhage, and Peter Görannson. Prediction and Measurement of Noise and Vibration Behaviour of Trimmed Body Components at Mid-Frequencies, Manuscript submitted for publication to *Applied Acoustic*, March 2009.

Paper B

Christopher J. Cameron, Per Wennhage, Peter Görannson and Sven Rahmqvist. Structural-Acoustic Design of a Multi-functional Sandwich Panel in an Automotive Application, Manuscript submitted for publication to *Journal of Sandwich Structures and Materials*, May 2009.

Contents

Part I

Introduction

1 Background

> **sustainable development** noun (a) *Economics*: economic development which can be sustained in the long term; (b) *Ecology*: utilization and development of natural resources in ways which are compatible with the maintenance of these resources, and with the conservation of the environment, for future generations.

The above definitions are taken from the Oxford English Dictionary, second addition [1]

Automotive History

The first production Model T, built by the Ford Motor company, was available to for sale to the public on October 1st, 1908. The model T was a car that changed automotive history, selling over 15 million vehicles over 22 years of production [2]. The model T was significant not because it was fast, quiet, or particularly comfortable, but because it was cheaper than its competitors, mass produced, and could be repaired and maintained relatively easily.

Figure 1: The 1915 Ford Model T

One hundred years after the first Model T, the automobile has become a method of transportation completely integrated into the infrastructure of developed countries and of increasing importance to the worlds developing economies [3]. Two significant influences on the development of the automobile have been the consumer and the regulating bodies. The automotive consumer has come to expect, among other things, improvements in performance, reliability, comfort, and fuel economy with each new vehicle. Governmental bodies around the world enforce safety and emission regulations like those of the UNECE in Europe, and the FMVSS and CMVSS in North America. Vehicle manufacturers must also generate a profit to both fund their research and development work as well as fulfil responsibilities to their shareholders. In order to meet all the demands of the consumer, fulfil the requirements of the regulatory bodies, and at the same time produce a net profit, the automotive industry is in a constant state of change.

Modern Vehicles

Over the years, consumer demand for options such as power windows, power steering, heated seats, and in recent years complex information and entertainment systems has lead to a steadily increasing number of components, and thus mass. The increasing electrification of vehicle systems leads to more wiring in vehicles, and increased demands on power systems, in turn making them heavier. Safety improvements also lead to increases in curb weight. Airbags and similar systems add mass directly while the contribution of energy absorbing deformation zones is less obvious. As you increase the amount of mass

Figure 2: A SAAB 93 Sport Combi (image courtesy of SAAB Automobile)

in a vehicle, the basic laws of physics dictate that you must increase the amount of energy necessary to move the vehicle. While modern combustion engines are much more efficient than their predecessors, if the mass of the vehicle consistently increases, the efficiency and power output of the engine must follow suit to obtain the same performance for the same amount of fuel.

Looking at some unofficial data [4, 5] as presented in table 1, it is rather obvious that an upward trend in vehicle mass exists. It should be stressed, that while data from vehicles

Table 1: Unofficial Vehicle Curb Weights of Saab cars 1950-2008

Model Year	Model Name	Curb Weight
1950-52	Saab 93	805 kg
0956-58	Saab 93	810 kg
0959-66	Saab 95	905 kg
1966	Saab 96v4	946 kg
1969-84	Saab 99	955 kg
1976	Saab 99EMS	1161 kg
1979-93	Saab 900	1174 kg
1984	Saab 900Turbo	1340 kg
1986	Saab 9000i	1280 kg
1985-98	Saab 9000	1302 kg
1988	Saab 900i	1285 kg
1999	Saab 9-3	1305 kg
2001	Saab 9-3Viggen	1438 kg
2004	Saab 9-3 1.8i	1440 kg
2008	Saab 9-3	1400-1600 kg

produced by Saab has been used, it is by no means the only vehicle manufacturer where this trend can be seen and it is rather doubtful that any vehicle manufacturer could produce figures showing the contrary. While advances in combustion engine technology have been significant through the decades, the fact remains that emissions are still produced in amounts directly related to the mass of the vehicle in question.

The ECO^2 Factor

In the past decade, an increase in world wide media coverage of climate issues has lead to an increased global awareness of the environment. International agreements like the Kyoto Protocol, adopted in 1997, place binding targets on pollution emissions of industrialized countries [6]. In October 2007, former United States vice-president Al Gore and the Intergovernmental Panel on Climate Change were awarded the Nobel Peace Prize for their work with man-made climate change [7]. The magnitude of these occurrences emphasize the increasing focus on the environment in recent years among governments of the world, the scientific community and the general public. These issues effect the automotive industry both directly and indirectly; directly via regulatory bodies that create and enforce more stringent environmental requirements, and indirectly via the very real demands of the automotive consumer.

Within the automotive industry, there is a great interest to meet and exceed the demands of the consumer and the governmental bodies in regards to all of their requirements. The

complicating factor is however that this cannot be done at a fiscal loss to the company or at a tremendous cost to the consumer, or the company (and possibly the consumer) will end up bankrupt.

Methods of producing what the consumer wants at a price they are willing to pay which fulfils or exceeds regulatory requirements are what the automotive industry is constantly searching for. Taking into account the desires of both the consumer and the vehicle producer to eliminate excessive waste, avoid depletion of natural resources, and minimize the impact of the vehicle on the environment and the resulting need becomes clear: methods of sustainable development are required.

Sustainable development, with respect to both economics and ecology within the automotive industry are the core elements of the work within this thesis. Specifically, methods of reducing weight, production cost, and production time of a passenger car whilst maintaining or exceeding engineering and consumer requirements and improving assembly ergonomics are examined. The methods proposed should have advantageous effects not only on the immediate factors (such as weight) but on secondary factors (such as fuel economy, styling, etc).

Specifically, noise vibration and harshness (NVH) criteria are investigated due to their importance to the consumer and their sensitivity to reduced weight and increased stiffness seen as necessary to achieve lighter, safer vehicles in the future.

Case Study

The work in this thesis examines the possibilities in reducing both ecological and economical footprints in vehicle production by combining the functionality of several traditionally separate components into a single multi-functional part. In this particular case, the roof system of a passenger car, from the interior trim to the exterior surface, is replaced by a single multi-layer, multi-functional sandwich construction. The methodologies developed attempt to fuse knowledge from several traditionally separate automotive disciplines into a singular toolbox for use with generic automotive design problems.

2 Automotive Noise Vibration and Harshness

Noise Vibration and Harshness

Noise, Vibration and Harshness, more commonly known as NVH, is an all encompassing engineering discipline that deals with the objective and subjective structural dynamic and acoustic aspects of automobile design. The NVH engineer is interested in the structural dynamic response of the vehicle from the complete assembled system down to the normal modes of the individual components. As a vehicle is a moving dynamic system, its response to stochastic, time varying inputs is important for safety, quality, and comfort of the passengers.

One specific area of study within NVH is vehicle acoustics. Sound plays an important part in the development of a motor vehicle. Certain aspects of noise produced by a vehicle are controlled by governmental regulations, for example pass-by sound levels or exhaust sound emission[8]. Other aspects of sound are controlled specifically within the individual company as a method of quality control. Meeting the constantly increasing, and complex needs of the consumer is also a key concern of the NVH program for any vehicle and deserves some specific attention.

Psychoacoustics in NVH

When a customer is deciding which vehicle to purchase, the overall quality of the vehicle is an important factor. This applies not only to the fit and finish of the bodywork, or the upholstery in the interior, but also to the sound and vibration behaviour of the car. Whether on an active or more subconscious level, customers pay attention to the sound quality of a vehicle, and it is an important by-product of design. Noise and vibration can have both positive and negative attributes; an irritating sound may cause the driver to become distracted, but engine noise and drivetrain vibration provide feedback on the operation of the vehicle. In addition the image of the brand can be effectively transmitted by the sound produced by the powertrain.

For a vehicle model to sell well, it is highly desirable to maximize the positive response and minimize the negative response to a given acoustic stimulus for a population of potential customers. The interpretation of what is positive and negative sounding to a customer is however a complex relationship. Studies have shown that the two similar sounding statements "This sound is annoying." and "I am annoyed by this sound." can have vastly different effects on the customers emotional state [9]. Objective NVH evaluation is difficult, if not impossible due to the unpredictability of the human senses. Genuit and Fiebig [10] showed that in a laboratory environment, visual stimulus can affect a persons interpretation of a vibrational or auditory stimulus. Terminology such as loudness, sharpness, roughness, fluctuation, strength and tonality are required within NVH to describe the quality of sound within a vehicle. The fact that perception and interpretation of a given noise varies between individuals and that a great deal of training is necessary to be a consistent and accurate at assessing noise, i.e. linking terminology to perception, is an ongoing problem within automotive NVH [11]. A great deal of work has been done attempting to link objective tests and subjective evaluations of sound and vibration. Attempts have been made to create standardized acoustic comfort scales using automated recording and evaluation methods [12], however at the present, it seems that the state of the art is not capable of emulating the human factor in the NVH equation.

The Physical Phenomena of NVH

NVH in passenger cars can be divided into two categories of interest [13].

- Noise: Audible sound in the frequency range 30-4000 Hz
- Vibration: Tactile vibration in the frequency range 30-200Hz

The three main contributors to interior noise are the engine and accessories, tyre/road interaction, and airflow over the external bodywork (wind noise) [14].

In a typical welded metallic body in white (BIW), noise transmission into the interior can occur along two distinctly different transfer paths; via airborne waves, or structure borne vibration.

Airborne Sound

Airborne sound often originates from external sources and propagates into the vehicle interior via holes in the bodywork, door seals, weld seams, etc [13]. Airborne sound propagation is predominantly in the higher frequency ranges. 80% of noise above 1000Hz is airborne in nature [15].

Controlling airborne sound can be done by eliminating the source of the sound (if possible), or eliminating the transfer paths into the vehicle. Increased sound pressure follows

the path of least resistance, and commonplace solutions such as acoustic baffles, urethane filler foams, rubber plugs and grommets, and adhesive seam sealants are used to impede an airborne sound propagating into the passenger compartment [15]. The implementation of these sorts of solutions rely heavily on testing, and experience of the engineers involved. For sound inside the compartment the absorption provided by soft, open structured materials can also be used to control high frequency airborne sound, this mechanism will be discussed in more detail in the section entitled "Porous Materials in acoustics".

Structure Borne Sound

Within a vehicles interior, 85% of noise under 500 Hz can be classified as structure borne sound [14]. Simply stated, structure borne sound is the result of mechanical vibrations causing localized displacements of air. Sound levels due to vibration can be directly related to the volume of air which is displaced. A 1 cm^3 volume displacement, which could be achieved by a 1 m^2 area of roof vibrating with a displacement amplitude of 1 μm, can cause a sound pressure of 75 dB in a vehicle interior [16]. Much of the noise in the frequency range up to 500 Hz is caused by cavity resonances which may be excited by vibrations of the body in white (BIW) caused by suspension or drivetrain inputs. The term booming noise is often used to describe acoustic phenomena in the frequency range below 250 Hz [17]. Body vibration levels are directly related to the road roughness, vehicle speed, suspension design etc. For a more complete explanation of the phenomena of structure borne noise in general, the interested reader is directed to [18].

Control of structure borne sound is primarily done by altering stiffness and damping characteristics of the vehicle structure or isolating a source from a receiving point. Structural stiffening may be applicable if vibrations are forced, damping when resonant vibration is the dominant issue, and isolation is useful where strong transmission paths exist and both source and receivers are stiff [19]. Stiffness is controlled by sheet metal thicknesses, geometry, weld points, etc. Damping, while also greatly affected by the joining method used, is primarily achieved using viscoelastic damping treatments. Constrained layer, free layer, and tuned viscoelastic dampers are often used on large panel surfaces, such as roofs, floors, doors, etc, to reduce vibration levels. The use of viscoelastic damping materials in the automotive industry is well documented [20] and experimental work to determine their size and placement, such as performed in [19, 21], is commonplace. Isolation is often used in motor and suspension mount design.

Computational Methods in Acoustics

Historically, NVH has been a manpower intensive process of "test-analyze-fix" [22]. Vehicle refinement often takes place in the final stages of production when designs are fixed and solutions to acoustic problems are far from ideal. In recent times, NVH has been making a progressive transition to computational methods and is taking a more preventative role in vehicle design.

Over the past 40 years, much work has been done attempting to predict internal noise in vehicles, primarily focussing on the frequency range 50-200Hz. This is the range where structure borne noise is dominant within the vehicle. A summary of this work can be found in [14]. Finite element analysis is the predominant method of choice within this frequency range. This is also the method primarily used within the work in this thesis. Other methods, such as statistical energy analysis (SEA) will not be discussed here.

One of the primary limiting factors in implementing FE in NVH analysis, has been the modelling of the interior treatments. Structural models are considered reliable and can be used, for example, to locate possible locations for surface damping treatments [23]. Capturing the frequency and temperature dependant damping properties of viscoelastic materials such as anti-flutter adhesives is however a more complicated matter which requires a rigorous testing program to evaluate the material [24]. While some tools and methods exist to simplify the validation of FE models with experimental results, the process is costly and time consuming and generally involves a lot of adjusting of the model to fit the test results [25].

A confounding factor in NVH analysis is the presence and influence of air. Unless testing is performed in the absence of air (i.e. in vacuum), the fluid surrounding a vibrating component will provide a certain amount of vibrational damping. The fluids effect on the global structural behaviour is often considered minimal, however in the case of resonant modes within the fluid cavity, this is not necessarily true. Accurate detailed modelling of the fluid cavity in the passenger compartment is not always performed, and for a large number of NVH calculations, the fluid is excluded from the calculations to limit calculation time. While computational methods like automated multi-level substructuring (AMLS) can greatly reduce the calculation time [26], achieving sufficient model fidelity to represent the phenomena at hand at the frequency at hand is always a problem. References [16, 27] give a rather detailed discussion of the subject matter which can be recommended to the interested reader. In linking the structural model to the acoustic media, the current state of the art utilities automated search algorithms to link structural elements to surround fluid elements [28, 29]. The control of these algorithms is not always simple and straightforward, and a degree of user skill is required in order to achieve the desired coupling and avoid unwanted coupling.

In a coupled fluid-structure problem, not only is the frequency of a resonant mode important, but also the phase. While a BIW may be capable of exceeding a given requirement, say the frequency of the first global bending mode, it is also necessary that mode shapes and phase of components of the BIW are of a certain nature. If for example, the roof and floor vibrate in a first panel mode out of phase (i.e. the "breathing" mode), there will likely be a problem with booming noise due to the compression of the fluid cavity. If the same vibration mode occurred in phase, the air compression may be minimal and no booming noise would occur. This sort of behaviour makes it important to understand the entire system, however the limitation in computational efficacy has meant that while full BIW analysis is possible, and in fact performed, full vehicle NVH analysis is still under development.

NVH engineering is very much a refinement process, and physical testing relies on the production of prototypes which can be very expensive. While computational methods can be used at any time in the design process, they often rely on a complete model being available for analysis. This is often due to the fact that global NVH behavior is significantly difficult to downward cascade to the component level [22]. While computer models are typically less expensive to produce than prototypes, waiting for a complete model of the vehicle until the final stages of pre-production means that a large number of the designs are fixed, and numerical analysis is implemented as a tool for "virtual firefighting" rather than for prediction and problem avoidance. The advantages of being able to use numerical methods from the beginning of the product cycle have been observed by many researchers and NVH engineers [30], restrictions in hardware, software, and a lack of methodology are the major restrictions at the moment.

Vibration and Acoustics in production vehicles

Often, NVH engineers strive to find an ideal solution for an acoustic or vibrational problem within a vehicle. Whether that solution is obtained by an intensive test scheme utilizing prototypes, or production vehicles, or whether the use of numerical methods is highly integrated, a common difficulty remains; namely the stochastic nature of NVH in production vehicles.

In recent years, several studies of large populations of production vehicles have been performed [31, 32, 33]. Results for these studies show the significant impact of minor differences in production on structural and acoustic NVH behaviour. Fluctuations in structural and acoustic frequency response functions may vary from 1 or 2 dB, up to 15-20dB, even for vehicles which should be identical [31]. These variations are not likely to be caused by some fault in the assembly process, i.e "lemon" examples, as few vehicles will deviate consistently from the mean population across the full frequency spectrum of measurement [32]. Instead, the variation in sound and vibration behaviour is attributed to a chain of very minor deviations within the assembly process whose sum is greater than the parts. Changes in such items as trim details, seat fabric, or carpeting will have a direct effect on the interior sound quality. For this reason, it remains a problem that any ideal solution arrived at with the help of physical or numerical experiments, will in fact be adjusted to fit exactly the prototype or model in question, and may be over, under, or poorly designed for the remaining vehicles within the population. While some effort has been made into developing a more statistical based approach to predicting NVH behaviour [33], their exists no complete solution at the current point in time.

Balancing Computation with Experiment

In the previous two sections, a description of the current limitations regarding computational methods of evaluating vehicle NVH experimentally have been given.

Difficulties in modelling the exact phenomena which occur in reality have been described. Finite element analysis is, in essence, solving a system of equations and so for the vast majority of finite element problems (exceptions such as buckling phenomena occur) there exists only one solution; i.e. it is a deterministic method. Arguably, it is not possible to recreate an exact replica of a phenomena observed in reality using a mathematical model as it will always include some sort of limiting simplification.

Regarding the experimental evaluation of NVH, it has been shown in the literature, and is a rather well known fact in industry, that the measurement of acoustic and vibrational characteristics of a vehicle can vary significantly even among vehicles which are identically constructed. Variation depends on manufacturing tolerances and environmental conditions, among a great many other things, but even the engineer performing the measurement is a variable. It has been argued that the exact same measurement performed under the exact same conditions by two different engineers would be different, if only subtly so.

This brings up the questions of what is it that FE should be used for in an NVH perspective? This is an interesting topic which has been discussed by, among others, Gartmeier [34, 34]. If the population of vehicles being produced can vary significantly in their NVH characteristics, what then is the purpose in attempting to duplicate the exact response of a single arbitrary example from the population? Finite element models, especially in the early stages of development, are capable of quickly establishing global characteristics for a new design, however while vast quantities of time and money might be spent on model refinement to mimic a given sample, the capabilities of that model in predicting the behaviour for the majority of the population may or may not be improved. The suitability of an experimentally obtained solution on a single vehicle may also be questionable for the other vehicles in production. Finite element analysis is an effective tool in NVH analysis, however the question of resource investment on refining and improving a model to represent an experimental "reality", which is in fact only one member in a statistically varying population should be asked. While the validation of mathematical models is essential, in an area such as vehicle NVH which involves a great deal of uncertainty, especially involving the human perception factor, perhaps "close" should be considered "good enough".

Porous Materials in Acoustics

Porous materials such as polymer foams, or fibre insulation, are capable of absorbing sound by converting the energy present in a sound wave into heat energy. The exact mechanism of the conversion process depends upon the geometry of the porous material as well as the frequency in question. The exact mechanisms of this absorption will not be discussed in detail within this work, and instead the reader is directed to [35].

Porous materials can be classified as a passive means of noise control. The efficacy of passive noise control is greatest at higher frequencies, perhaps in the region of 1000 - 3000 Hz [36], however they are still capable of providing significant noise reduction(i.e. greater than 10dB) above 125 Hz. Many modern cellular foams are created from polymeric

materials by the use of chemical blowing agents [37] and it is possible to vary the size and geometry of their cellular construction. Altering the size and cell type of foams affects their acoustic properties [38], as well as combining layers of different kinds. Historically, the effectiveness of a given foam or combination of foams at absorbing sound energy has been measured experimentally, as for example in [39].

Within the work in this thesis, numerical methods are used to model the elasto-acoustic properties of porous solids in an NVH application. Calculations are performed using commercially available numerical codes [40] in addition to in-house hierarchical finite element solvers. The exact models used are explained in [41, 42, 43, 44] and are not included here.

3 Sandwich Structures

The Basic Sandwich Structure

A structural sandwich, in its most basic form consists of two stiff, strong and thin sheets bonded to either side of a relatively thick, weaker, lightweight core material. Figure 3 shows a schematic drawing of a basic sandwich structure.

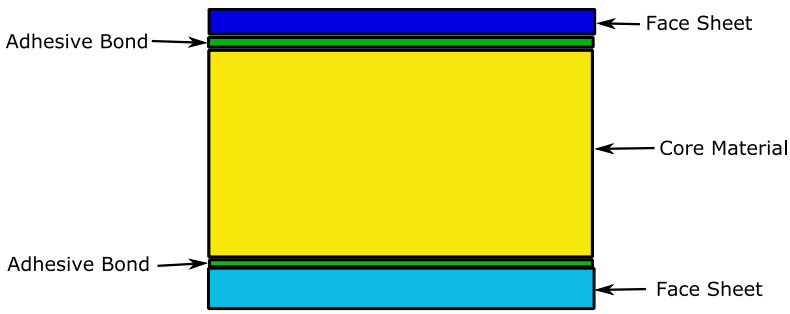

Figure 3: A basic sandwich construction

The most common face sheet materials in structural sandwich components are metals or fibre reinforced plastics. Common core materials are expanded foams of PVC, PET, or other plastics, honeycombs of aluminium or resin infused paper (Nomex), or balsa wood. The face sheet layers in a sandwich structure carry applied bending loads and moments as tensile and compressive stresses while the core material carries transverse loading predominantly as shear [45].

A monolithic construction of unit width and thickness t, as depicted by the uppermost beam in figure 4, will have a certain stiffness in bending which can be normalized as 1. In sandwich terminology, this bending stiffness is also called flexural rigidity. By splitting thickness t and separating the two halves with a lightweight core material, the bending stiffness can be increased without greatly increasing the weight. By the same method that the stiffness is increased, so is the bending strength of the sandwich, i.e. the loading level at which failure in bending will occur. The relative increase of flexural rigidity and bending

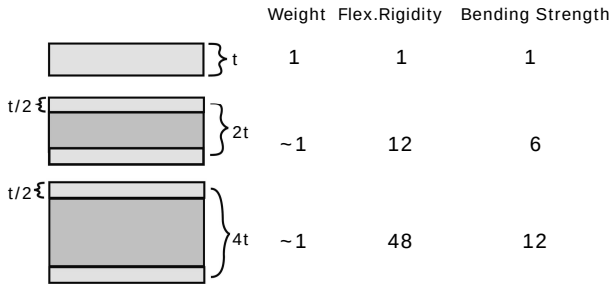

Figure 4: The sandwich effect (courtesy of Zenkert)[45]

strength is shown for a two fold and four fold increase of sandwich thickness for the same thickness of face sheet material t in figure 4. Core material is assumed to be of a much lower density than face sheet, and thus the additional mass does not contribute significantly to the mass of the construction.

The deformation of sandwich structures is not only controlled by the bending stiffness, but also by the shear effects. As face sheets are usually quite thin, they present little resistance to bending moments; at the same time core materials are relatively weak and can relatively easily be deformed by in-plane and out-of-plane stresses due to the applied loads. Shear stresses and deformations, usually ignored in problems where monolithic structures are subjected to bending loads, contribute considerable to the response of a sandwich structure subject to the same loading scenario. In the bending of sandwich beams, the contribution of both pure bending and shear deformation must be accounted for. As mentioned in [45], the effects of these shear deformations are not always obvious, and may surprise the inexperienced analyst.

Applications of Sandwich Structures

Stiffness in bending is only one aspect of what a sandwich panel can provide. By varying the face sheet material and the core material properties, characteristics such as sound absorbance, damping , corrosion resistance, recycle-ability, density, and sensitivity to out-of-plane loading, to name a few, can be altered to suit the desired application. The sandwich construction offers a great deal of flexibility in design for a minimized weight penalty.

Despite their many advantages, sandwich constructions are not infallible, and not necessarily always the correct choice for certain applications. Sandwich structures in general are poorly suited to concentrated out of plane loading which can lead to core or face material failure and failure of the structure. To an engineer working with sandwich construction, phenomena such as face sheet buckling, global buckling, core shear failure, face sheet delamination, and adhesive layer failure must be understood to construct a robust structure.

Special design consideration must be taken when introducing loads into a sandwich structure or when creating a joint between two sandwich panels due to stress concentrations an other effects [46].

The aforementioned points need not prohibit the use of a sandwich structure in a given design, but are given to emphasize the necessity of detailed knowledge of the subject matter by the design engineer. For further explanation, the interested reader is directed to [45], the primary resource for sandwich information used within this work (and for a great many sandwich structure engineers!).

Sandwich Structures in the Automotive Industry

While a great deal of literature on sandwich structures describes the potential for their use within vehicles and development of tools to ease their implementation has been ongoing since at least the mid 1980's [47], the use of pressed and spot/laser welded steel structures is still the praxis within the automotive industry. Very little published work exists describing full scale mass production of automobiles which use sandwich structures as load bearing or structural components. The primary reason for this, according to the literature, is cost; should a new material be used to replace an old, its entire cost including raw material, manufacture, design, and development must be less than that of the material is should replace [48]. While the raw material costs of sandwich structures are generally higher than their steel equivalents, this is not the major cost which has prevented the full scale implementation of sandwich structures in automotive production.

Computational simulation is heavily relied upon to predict and optimize high and low speed impact behaviour of vehicles to meet stringent government safety requirements on frontal and side impact, and rollover (among other things) [49, 50, 51]. Modelling techniques and material models for use with metallic construction have been developed over decades and are tested and reliable. The same cannot be said of the modelling methods of typical sandwich structures in crash. Even the simplest sandwich construction using a metallic face sheet and a polymer foam core becomes a very complex problem when attempting to predict face-core de-bonding, or buckling phenomena, particularly when dynamic loading is involved. Experimental methods are often necessary to asses the crashworthiness of sandwich structures [52]. As the current state of the art in finite element analysis is not capable of consistently predicting the crash behaviour of sandwich structures, increased use of sandwich structures in the automotive industry would necessitate an increase in prototype based crash tests for development and validation. While in the long term, this would no doubt lead to a better understanding of the behaviour of sandwich structures in impact, and much improved modelling techniques, in the near term it would be a substantial cost.

Manufacturing costs are also of interest. Existing methods for sandwich construction usually involve much lower rates of production and are significantly less automated than those used in the automotive industry. On the other hand, the cost of high quality tooling for a

composite based sandwich structures is a fraction of that for high quality steel stamping tools. The lowered cost of tooling offers added benefit with respect to styling; as tooling costs less, it may be switched out more often and changes in design can be achieved quickly. Using conventional methods of production, the only possible way to achieve the production rates necessary would be to introduce more production stations. Determining at which point the balance between production rate, tooling/material/personnel cost, and production area requirements/costs exist is beyond the scope of this thesis, but is an interesting area of speculation. New methods of production are being developed which show promise [53], and it is likely only a question of time and resources before satisfactory production rates and levels of automation sufficient for the automotive industry are achievable. Sandwich constructions also have the potential to eliminate problems of corrosion and increase the lifetime of components, provided they are designed and manufactured correctly. While this may be of questionable interest to the vehicle manufacturer, as they wish to sell more vehicles, the interest of the consumer in a product that is more durable and has a longer lifetime may be worth more so as to compensate for the reduced sale in new vehicles; this is however purely speculation at this point in time. In 1995, when the use of aluminium and magnesium was becoming increasingly popular for automotive applications, a cost per kilogram weight reduction of less than $2 U.S. was required for a new material to have a good chance of being implemented in a new design [48]. While it is unknown at the moment how that figure has changed since, the influence of environmental costs has no doubt contributed to its increase. Already we are seeing that the significant use of composite materials and sandwich structures is possible in automotive applications, even if they are somewhat extreme in nature [54]. The question remains as to how long it will take until this technology becomes accepted, or even encouraged in more mainstream automotive engineering. The potential for the technology to yield solutions for the industry is perhaps only limited by the possibilities of the industry to provide solutions for the technology. Time, and money it seems, will determine what happens next.

4 Optimization

Basic Optimization Theory

Optimization,within the context of this thesis, refers to an iterative process in which an equation or set of equations is solved to minimize a certain quantity most often with a set of mathematical constraints placed on the unknown variables. The basis for successfully solving an optimization problem is a well described mathematical expression of the quantity to be optimized, commonly known as the objective function. One or more unknowns, called design variables, must be given which are allowed to be altered by the optimization algorithm to achieve a best possible value of the objective function. Constraints are envelopes within which certain parameters are valid, such as the values of the design variables or a result from a calculation. Equation 4 shows a basic optimization problem where $f(x)$ is the objective function, x_1 and x_2 are the design variables, and the inequalities for $G(x)$ represent the constraints.

$$\begin{aligned} \text{minimize} \quad & f(x) = x_1 + x_2 \\ \text{subject to:} \quad & \\ & G(x_1) \geq a \\ & G(x_2) \geq b \end{aligned} \tag{1}$$

Each iterative loop in an optimization should yield an improved value of the objective function, and valid values of the parameters on which constraints are placed. For a detailed explanation in optimization theory, the interested reader is directed to [55].

Computational Structural Optimization

Structural optimization can, generally speaking, be broken into three separate categories: size optimization, shape optimization , and topology optimization [56]. In size optimization, dimensions of the various components are used as design variables, for example sheet metal thickness. Shape optimization alters the geometric boundaries of the structure to

achieve an optimized solution. Topology optimization uses the presence or absence of material at a given point as the design variable to achieve an optimized configuration.

The case study in the work performed in this thesis can be classified as a shape optimization with several design variables and a single objective function. A component of sandwich construction is to be designed which shall be as light as possible but must uphold a certain level of performance. The objective function for this problem is the weight of the panel. Thickness of the individual layers of the panel are the design variables. Constraints are placed on the optimization by limiting deformation under load and the frequencies of the normal modes of vibrations. The problem is a twofold numerical problem, finite element analysis calculations provide input to the numerical algorithm for the iterative optimization loop.

The first step in solving a given optimization problem is to select a suitable algorithm. The choice of algorithm will depend on the type of problem at hand, the number of design variables, the nature of the objective function, and the computational cost involved with each. For a single variable objective function with a continuous derivative, gradient based methods may be the most optimal. If the objective function is highly stochastic, has discontinuous derivatives, or is a multi-objective function, different algorithms may be necessary or prudent for computational efficiency. In 2008, Duddeck [57] performed an evaluation of a number of optimization algorithms for multi-objective design optimization within the automotive industry. Conclusions of this evaluation were rather simple; for linear problems, like basic NVH global stiffness and normal mode problems, gradient based methods are effective. More complex problems, especially those with multi-criteria objective functions require optimization schemes more capable of finding a global, rather than local optima.

While algorithm efficiency is important, the single largest problem in numerical optimization is the computational time required to evaluate a single loop in the optimization cycle [58]. Improvements in CPU speed, memory capacity, and software capabilities have reduced the total cost of computer based optimization roughly one billion (1 000 000 000 000) times since computer based optimization began in 1971 [59]. Despite this fact, over the past decades, the time required for performing a specific type of calculation has not drastically improved and remains around the region of 12-20 hours. This can be attributed to two different factors of complexity; modelling and analysis.

The problem with analysis is rather simple. In many cases, there exist problems where the most well developed implementations of mathematical models are not capable of explaining or modelling the observed phenomena. As new models are developed, or existing models adapted to solve these problems, the computational time generally increases to solve the problem. It may even be that in order to gain a better understanding of a problem, an analyst may change to a more accurate, and usually more complex form of analysis; for example from linear to non-linear solution sequences within FE [59].

Demands on model fidelity increase according to the demands of the analyst and the capacity of the computational arrays available. Currently, a characteristic element length of approximately 10 mm is considered sufficient for many applications. Smaller element size

often yields increased accuracy, especially in regions of stress concentrations. Element size also is a controlling factor in the frequency limit of a dynamic analysis; a finer mesh will provide reasonable results to higher frequencies. No intelligent computational analyst would refuse a more refined FE model if it were capable of being computed in the same or less amount of time. This amount of time is however directly related to the computer hardware available.

Kodiyalam *et al* describe a state of the art computational array in 2004 having 128 CPU's, each 400 MHz, with a total of 131 GB of RAM [60]. Numerical calculations within this thesis were performed on a single workstation using 4 processors, each 3.14 GHz using 16 GB of memory. While the number of processors and amount of memory used in this thesis are dwarfed by the array used in [60], the speed at which a single binary calculation can be made has increased by a factor of eight. The ongoing conflict between Moore's law[1] and Parkinson's Law[2] however likely means that while technology and software improve, time will always be the governing constraint on optimization problems.

Assuming then that the total amount of time used for optimization is somehow held constant, it is perhaps interesting to look at the current method for dividing up calculation time between different areas of study. Crash and impact simulation is, without question, the single most computationally expensive area in vehicle design; this is an opinion unanimously agreed upon by all sources found in the literature [56, 57, 59, 60, 61]. Crash optimization using modern, efficient algorithms, such as latin hypercube sampling, requires 3 to 4 calculations for each design variable [61]. Given that each calculation can take between 12-20 hours, it can easily be seen that several weeks may be required for even a moderately simple optimization problem. It is a general default that NVH optimization is included simply as a constraint on global bending stiffness of the BIW and a restriction on the frequency for a resonant mode of vibration. In none of the literature on multi-objective optimization was an NVH analysis performed using a full cavity FE model. Given the number of constraints on crash behaviour, it is perhaps not an unexpected trend, however, it can be expected that as with all other areas of numerical computation, the level of intricacy of NVH optimization will increase as hardware and software allow.

The problem of long computational times is hardly a new issue, and different approaches at minimizing its effect on the design process have been developed. In large FE problems substructuring-i.e. breaking a single large model into several interconnected small models- is often used. A very well known and effective method called automated multilevel substructuring (AMLS) is used a great deal within the automotive industry and has been proven to both speed up calculation times and enable accurate results up to higher frequency ranges within a given length of time [62]. For the optimization of a single component within a body in white, the use of super-elements has also been explored [63, 64].

[1] In 1965, Gordon Moore, founder of Intel, stated that the number of devices on a silicon chip would double every 18 months. This is commonly known as "Moore's Law" [59]

[2] In 1959, Cyril Northcote Parkinson published an essay in "The Economist", the opening line of which was: "It is a commonplace observation that the work expands so as to fill the time available for its completion". This statement has become more commonly referred to as "Parkinson's Law"- C.Northcote Parkinson, The Economist, November 1955

So far, within the literature, limited work has been done on full scale optimization of coupled fluid structure systems, especially those with acoustic objective functions, except for rather geometrically simple problems [65]. This is largely due to the increased number of degrees of freedom due to the fluid cavity in addition to the added computational difficulty in solving a coupled fluid-structure problem. While new methods of dealing with this problem are being developed [27], the current state of the art in coupled fluid structure analysis lacks the number or refinement in numerical tools compared with structural analysis by itself.

Within an industrial context, in addition to all of the absolute time constraints caused by model size, and computational issues, there exist a great many practical points of interest that are perhaps relevant to discuss. Regardless of the efficiency of the models and computers, engineers must be involved in the process to achieve results that are meaningful [66]. There also exists the problem of transposing a global design objective which is of interest, to a more localized design requirement which can be optimized [67]. As an optimization problem seeks to include more areas of interest, it requires the input of more groups of experts which are often located at least at different areas within the company if not at different locations around the world. While a single analyst may be capable of carrying out a simple multi-disciplinary problem, complex refined problems will require more than a single individual [58]. These sorts of organizational problems can also be costly, but the cross-competency interactions can also help to develop new areas of study; for example including fiscal or environmental impact factors in the structural design process [68]. In the end, it must also be remembered that in an industrial context, the exact optimal solution is not of interest, it is instead a sufficiently good solution that can be reached in a minimal amount of time which is the goal.

Optimization within this work

The method of moving asymptotes (MMA) [69] was chosen to solve the optimization problem assesed in this work. MMA was chosen for the following reasons:

- MMA is well suited for solving structural optimization problems.
- Experience and Competence in using MMA exists within the research group.
- MMA was available in an easily implemented software package available within the division of lightweight structures.

Specifically, the program Xopt developed and provided by Alfgam Optimering AB[3] was used.

[3] www.alfgam.se

5 Summary of Work Performed and Discussion of Results

The previous chapters within this thesis have given a background in the areas of vehicle NVH, sandwich structures, and optimization. This chapter will position and explain some details of the work performed and its contribution to the body of scientific knowledge in the field.

The research work leading to this thesis forms a synthesis between design of a structurally viable component and its acoustic performance. The paradigm used is multifunctionality, i.e. designing an integrated component with desired acoustic and structural performance at a low weight.

To establish a datum baseline, an initial campaign involving testing and simulation of a state-of-the-art vehicle component (in this case, the roof system of a passenger car) was performed. The results from this work formed the starting point for the actual design optimization, leading to the new, integrated concept derived having lower weight, comparable performance, and lower level of complexity.

Baseline Characterization

The testing and simulation work to establish the current state-of-the-art involved several steps. Initially, full-vehicle acoustic measurement of a production Saab 9-3 SportCombi was performed. Following this, the roof structure of the same production vehicle was removed and sent to KTH where laboratory measurement of acoustic and vibro-acoustic properties could be performed. Sound transmission loss (STL) testing was performed for both the full vehicle, and for the component according to international standards.

Comparison between the results of STL testing for full vehicle and component testing showed extremely good agreement as can be seen in figure 5. Two significant conclusions which can be drawn from the acoustic testing results are as follows:

- With regards to sound transmission loss testing, for the roof panel at least, and most certainly for other body panels, in-situ testing yields sufficiently accurate results as

to eliminate the need to disassemble a vehicle to measure individual components.

- In frequencies above approximately 1000 Hz, sound transmission through glass surfaces contributes significantly to the total sound transmission into the passenger compartment.

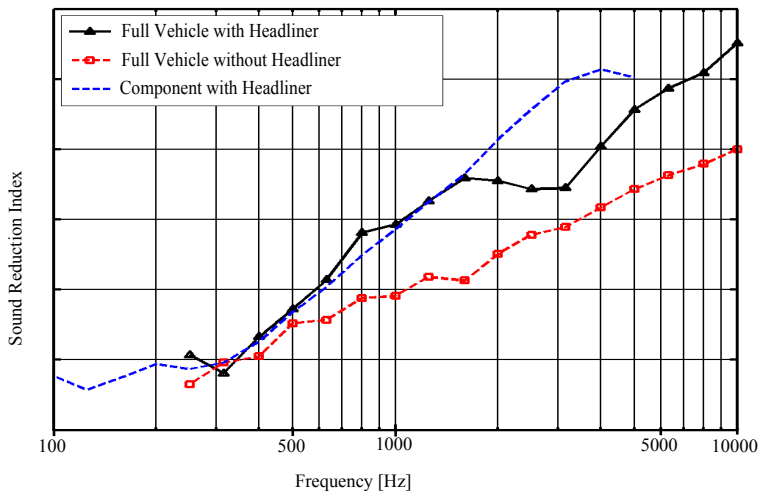

Figure 5: Sound transmission loss comparison

In addition to sound transmission loss testing,vibro acoustic testing on the roof component was done to measure structural frequency response for a forced excitation. An inertia shaker was attached to the drivers side A-pillar and excited using a white noise signal. A laser vibrometer was used to measure the vibrational velocity of a set of grid points on the inner headliner and outer roof. Figure 6 shows the shaker setup and measurement points.

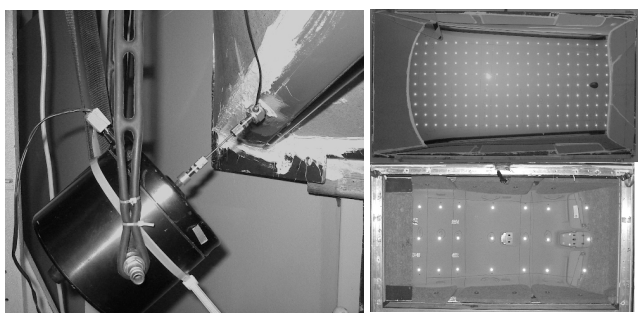

Figure 6: Inertia shaker attachment and measurement grid points

Table 2: Mechanical properties of headliner components

	Young's Modulus[MPa]	
Component	Testing	Literature
Outer Membrane	9100	4500-7500
Inner Membrane	4800	4500-7500
Foam Layer	8.80	3.45

For the baseline configuration, tensile testing of the material in the vehicles headliner was performed in order to fully characterize its properties. Testing was performed according to international standards [70] using equipment available in the lightweight structures laboratory at KTH. The headliner, as illustrated in figure 7, was composed of three structural components; two fibre reinforced plastic membranes, and a cellular foam core assumed to be polyurethane based. A total of ten samples of each structural layer were tested to obtain Young's modulus. Tensile testing of the structural foam, while not ideal, was the only method available given the limited amount of material and its geometry. The values of stiffness for the various layers were compared with values within the literature and found to be reasonable, if somewhat above expectations. Table 2 shows the results of tensile testing compared to values within the literature.

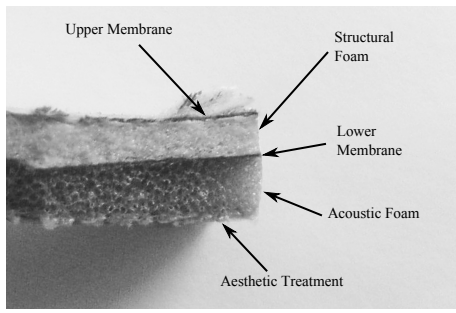

Figure 7: Closeup of headliner cross-section

Complimentary to the testing, numerical simulations were performed. The intention of the numerical simulations were to develop and verify a methodology which could be later used in the design optimization process. This was achieved through two fundamentally different modelling approaches, one focused on realism, i.e. true geometry, and one focused on accuracy and computational effort, i.e. simplified geometry. In the baseline configuration, the headliner was of specific interest.

The headliner is in itself, a multi-layer component, however as the focus of the work was on a more global structural-acoustic level, a simplified method of modelling the headliners properties was developed. This was achieved using the results in table 2 together with basic sandwich theory.

For a sandwich structure, the Young's modulus through the thickness varies depending on the material layer. Figure 8 shows the cross-section for an arbitrary sandwich with dissimilar faces, as was the case for the headliner.

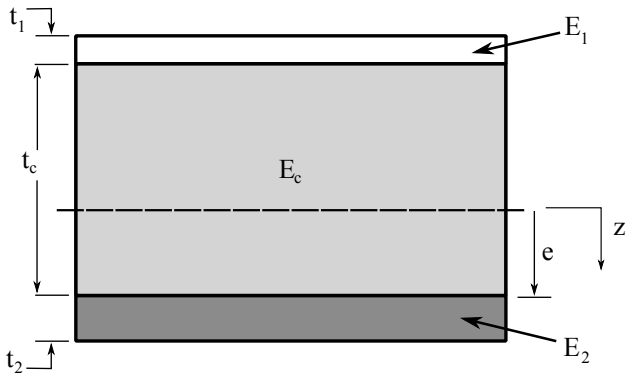

Figure 8: Arbitrary sandwich cross-section (redrawn from [45])

Flexural rigidity (denoted as D), which describes a sandwich beams stiffness in bending, can for a unit width sandwich beam of arbitrary cross section (see figure 8) be expressed in the following manner [45]:

$$D = \int Ez^2 dz = \frac{E_1 t_1^3}{12} + \frac{E_2 t_2^3}{12} + \frac{E_c t_c^3}{12} + E_1 t_1 (d-e)^2 + E_2 t_2 (e)^2 + E_c t_c (\frac{t_c + t_2}{2} - e)^2 \quad (2)$$

Where:

$$e = \frac{E_1 t_1 d}{E_1 t_1 + E_2 t_2}$$

$$d - e = \frac{E_2 t_2 d}{E_1 t_1 + E_2 t_2}$$

$$d = \frac{t_1}{2} + t_c + \frac{t_2}{2}$$

Lower case t denotes a thickness, and E is the Young's modulus. Subscripts 1 and 2 denote the upper and lower face sheets. Subscript c denotes the core material. In this case, the face materials are the two fibre reinforced membranes and the core the polyurethane foam layer. Lower case z denotes the vertical coordinate of the sandwich cross-section where $z = 0$ is the neutral axis of the sandwich structure. By inserting values of t and E into Equation (2), a value can be obtained for the flexural rigidity.

The thickness of each of the components comprising the headliner were measured at a number of locations, and average values for each layer were inserted into equation 2. Thickness variations were primarily within the urethane foam core, most likely an effect of the manufacturing process which often involves press forming [71].

Using a total nominal thickness for the entire headliner of 6.0 mm , an equivalent Young's modulus was obtained for use in the FE model according to equation 3. Density of the model was based on measured mass of the headliner.

$$E_{equiv} = \frac{D}{\int z^2 dz} = \frac{D}{\frac{(6.0)^3}{3}}[MPa] \tag{3}$$

These methods enabled the entire headliner to be modelled without detailed modelling of the individual layers which was of sufficient accuracy for the work performed within this thesis.

Using a hierarchical finite element code developed in house (and explained in detail in [41, 42]), sound transmission loss calculations for the roof structure with equivalent headliner properties were made through the frequency range of 100 Hz to 1000 Hz and compared to the aforementioned testing. Results can be seen in figure 9. The conclusions of this comparison is as follows:

- Hierarchical FE modelling using the equivalent solid methodology is accurate in predicting sound transmission loss up to approximately 500 Hz.
- Above 500 Hz, the simplicity of the model prevents the accurate prediction of sound transmission loss; this is mainly related to the excitation method.

In addition to hierarchical FE analysis, coupled fluid-structure analysis using Nastran was performed. A model of the headliner was created using the equivalent mechanical properties. Damping properties of the headliner were calculated based on material properties of the acoustic foam layer and on theories for acoustical wave propagation within porous media which can be found in the literature [35]. A structural model of the component tested in the laboratory was created as was an acoustic cavity model accounting for the headliner. A cross-sectional view of the FE model can be seen in figure 10.

The model was excited in the same manner as in laboratory test, i.e. a harmonic excitation was applied to the drivers side A-pillar, and vibration velocity levels of the headliner

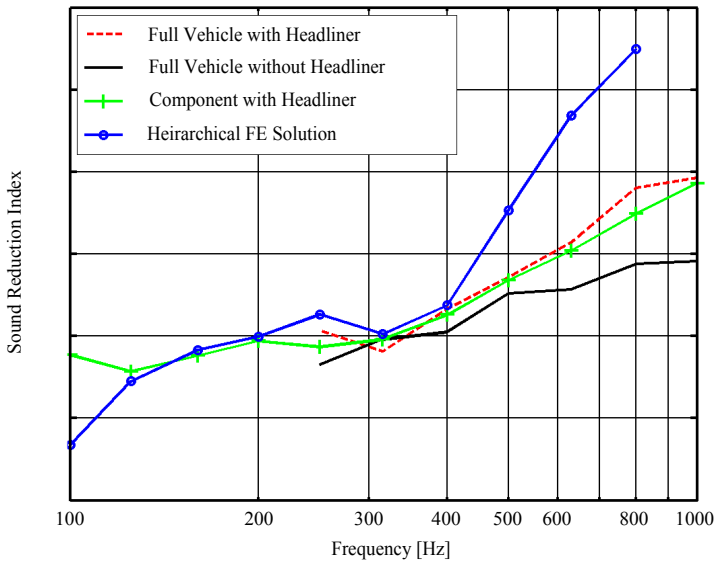

Figure 9: Measured and numerical sound transmission loss in 1/3octave bands

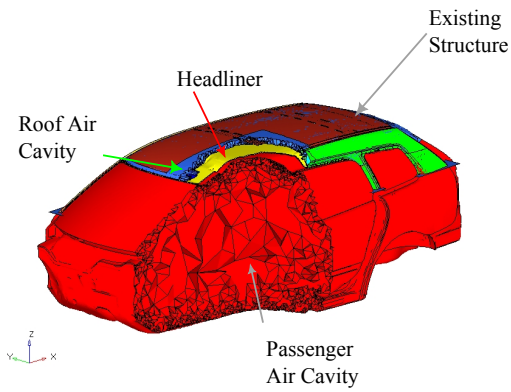

Figure 10: Cross-section of FE model

and outer roof were calculated. A basic parameter study was also performed using the FE model to evaluate the effects of headliner stiffness and boundary condition variations on the vibration levels of both the headliner and the outer roof. In comparing results from vibroacoustic testing with calculations using the Nastran model good agreement was obtained. Figure 11 shows one such example of comparison between measurement and finite element calculations.

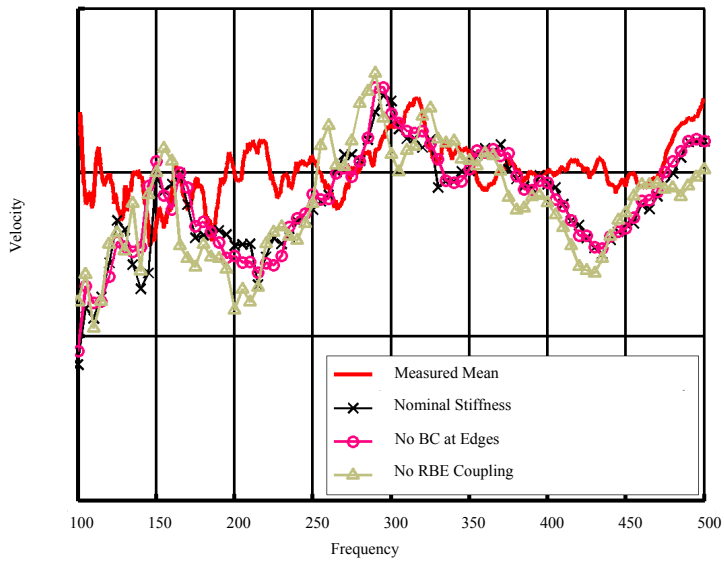

Figure 11: A comparison of FE and vibroacoustic testing results

In comparing the FE results to testing results, the following conclusions were made:

- The mechanical coupling between the roof structure and the headliner has the largest impact on the vibration level of the headliner among the parameters investigated.
- Stiffness properties of the headliner have relatively little effect on its vibrational behaviour

As the headliner in a vehicle interior is a large surface in direct contact with the air surrounding the vehicle occupants, its vibrational behaviour is significant to the level of sound within the cabin. Should such a design be used, from an acoustic standpoint, a better understanding of the nature of the attachment mechanism would aid in NVH development.

While the above points are important, the single largest contribution to vehicle NVH analysis is as follows :

> The method of modelling, using equivalent properties, while simple, proved to be accurate from a vibro-acoustic standpoint. Modelling of interior trim components using three dimensional finite element models is still in its infancy for both academic and industrial applications. This observation is based on a thorough literature survey and discussions with experienced individuals in

industry. Accounting for the acoustic and vibrational aspects of interior trim by modelling the actual components is the next frontier within vehicle NVH and offers a powerful tool for prediction during design.

In addition to being quite accurate, in particular concerning the higher frequency range, the modelling methodology developed was simplistic enough that implementation for other trim panels of interest should not be exceedingly difficult. In addition , the work within this paper has contributed to extend the understanding of coupled structure-acoustic analysis using finite elements in the mid-frequency range.

Introduction of Multifunctional Sandwich Concept

In the second part of the work, a new concept for a roof system was proposed in which all components from the outer sheet metal to the interior trim were replaced by a single multi-functional sandwich panel. Figure 12 gives a graphical representation of the concept.

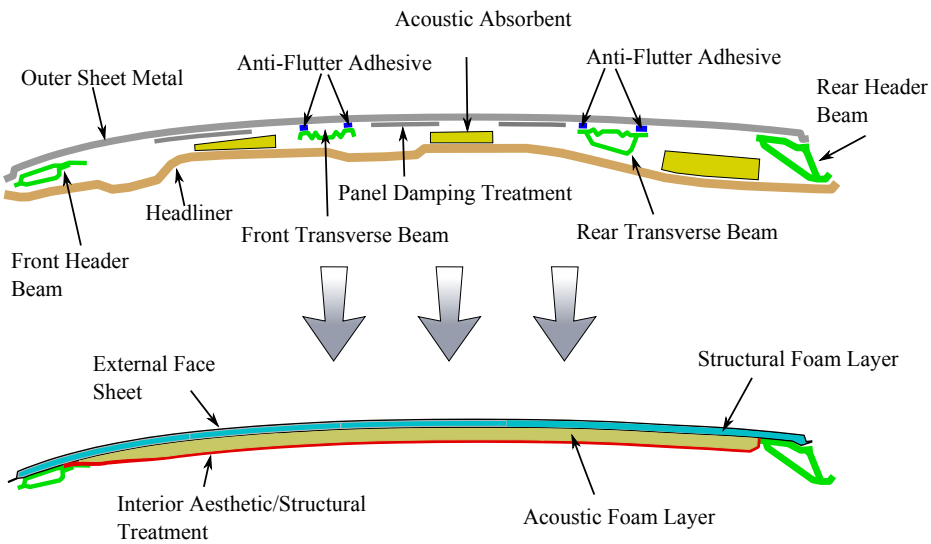

Figure 12: A schematic of traditional and sandwich panel design

Two configurations of the concept were proposed, each consisting of four components; external face sheets of isotropic material, a structural foam layer of typical polymeric sandwich core foam, a single layer of lightweight, open–celled acoustic foam , and an interior face sheet which provides both structural and aesthetic functionality (see Figure 12). In one panel configuration, the interior face sheet was perforated to allow fluid interaction

Table 3: Material properties in FE model for sandwich panels. In cases where properties differ, perforated values are shown inside square brackets

	Outer Sheet	Struct. Foam	Ac. Foam	Inner Sheet
Material	Aluminium	Closed Cell Foam	Open Cell Foam	Aluminium
E (MPa)	70 000	135	0.10	70 000 [46 460]
G (MPa)	26 000	35.0	–	26000 [–]
ρ (kg/m^3)	2710	100	30	2710 [2170]
ν	0.3	0.4	0.1	0.3 [0.27]

between the passenger cavity and the acoustic foam, thus providing sound absorption in the interior of the panel. A fixed rectangular hole pattern was assumed with holes 2.0 mm in diameter and 4.0 mm centre to centre spacing. For numerical purposes, a method was derived from the literature [72, 73] to model the perforated plate with equivalent solid properties. Table 3 shows the values of material data used in the optimization.

Both configurations of the panel were optimized to a set of structural constraints obtained via engineering specifications and finite element analysis of the existing design. Results for the objective function, design variables, and active constraint can be seen in table 4.

Table 4: Optimization results for perforated and non-perforated panels

	Perforated Panel	Non-Perforated Panel
Optimized Mass(% of Conventional)	17.643	18.215
t Outer Sheet [mm]	0.200	0.200
t Structural Foam [mm]	5.088	4.6004
t Inner Sheet [mm]	0.200	0.200
Active Constraint	Local static disp.	Local static disp.

The structural optimization performed was, in itself, not entirely remarkable; established optimization algorithms were used, as were somewhat standard forms of static and structural dynamic constraints. In establishing the requirements, the difficulty in translating global requirements to component level requirements was emphasized, as was the need for improved understanding in this area. Two interesting points that were established from the results are the following:

- For the examined structural constraints, the existing construction is tremendously mass-inefficient due to compromises between requirements of design and production
- Robustness required for everyday use may in fact be the limiting factor for minimum weight when replacing a steel structure with a sandwich structure

After structural optimization, the two configurations of the sandwich component were evaluated using advanced finite element analysis software for poro-elastic acoustic calculations. The software CDH\EXEL[4] in conjunction with NXNastran 6.0 was utilized to perform coupled fluid-structure analysis. Frequency response analysis was performed using a single fluid cavity of identical exterior shape as that used for the conventional solution. Both the conventional and sandwich panel models were excited in the same manor, namely a single node inside the fluid cavity located approximately at the drivers head was excited and the average fluid pressure within the cavity was calculated for the frequency region 100-500 Hz. Results of the calculation can be seen in figure 13.

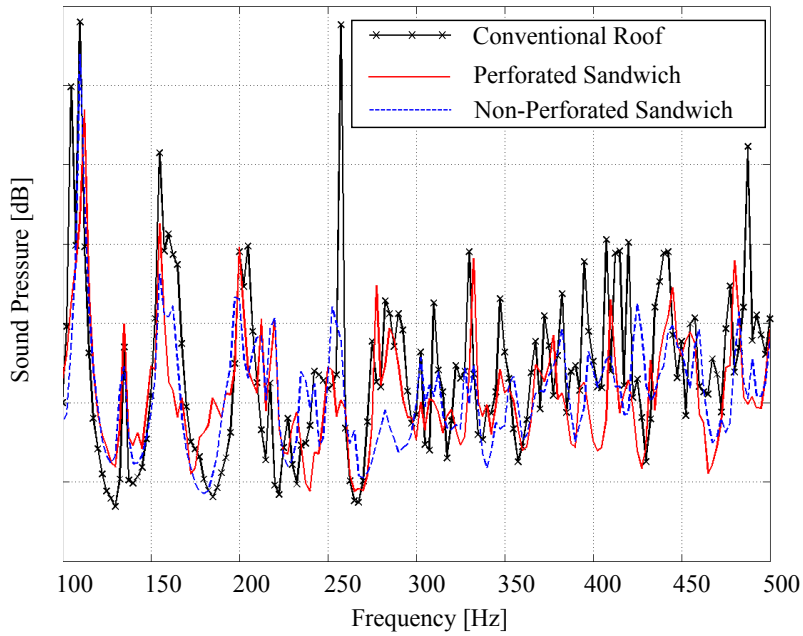

Figure 13: Average sound pressure in cavity vs excitation frequency (Y-Axis 5 dB steps)

The results in Figure 13 showed that the general behaviour of all three configurations was quite similar. This result was, from an acoustic standpoint, very significant; despite the fact that mass of the system has been reduced by approximately 80%, no noticeable degradation of the acoustic environment has taken place.

Figure 14 shows the same results as obtained in Figure 13, however levels have been averaged over 10 Hz intervals. Here, the differences between the conventional and sandwich configurations is much clearer. It can be seen without doubt that no degradation of the

[4] http://www.cdh-ag.com/de/exel.html

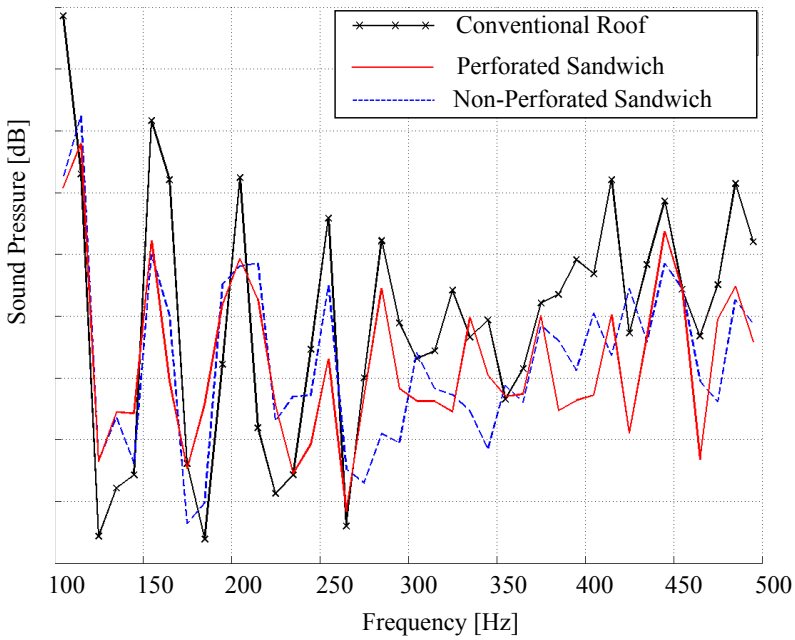

Figure 14: Average sound pressure in cavity vs excitation frequency [Averaged over 10Hz] (Y-Axis 5 dB steps)

acoustic performance has taken place in spite of the significant reduction of mass. It would also appear, that in the frequency range above 300Hz, the sandwich constructions in fact may perform better than the conventional design. Differentiating between the perforated and non-perforated configuration is somewhat more difficult. At some frequencies the perforated panel appears to perform better, and at others the non-perforated. This observation brings up an interesting point of discussion; while the non-perforated panel represents a minima in acoustic absorption, the perforated configuration, which was rather arbitrarily chosen, offers potential for improvement in absorption characteristic.

The final results of the work in this thesis yield a component that meets the structural targets without degrading acoustical performance, but is of questionable robustness and which proved impossible to produce with conventional methods. While this result is in itself uninteresting, being merely an academic proof of concept, the major contribution to vehicle NVH from the work in can be described as follows:

> The proposed concept offers a new idea within the area of sound and vibration control within an automobile. Heavy and inefficient visco-elastic damping treatments, insulation, and aesthetic treatments have all been replaced by

> the use of a more intelligently designed structure offering integrated damping via the use of structural and acoustic foam elements. Utilizing the sandwich concept to obtain maximum stiffness for minimum weight results in large reductions in mass while still meeting the same structural criteria, and without degradation of the acoustical environment.

While the final panel is not suitable for production, this work provides a proof of concept and a strong argument for further investigation and optimization.

Further Implications

Using some creative thinking, it is quite possible to create a long list of potential areas of improvement a modular sandwich based construction could achieve for the case studied in this thesis. The potential for a significant reduction in the mass of the roof system is obvious. An improvement in the acoustic properties of the interior should also be achievable. While it is explicitly within these two areas that improvements can be quantified with exact numbers and numerical results at present, a number of other areas would however be affected directly as a result of the switch to a modular sandwich construction.

Among other things, it is reasonable to presume that improvements within the following areas should be attainable:

- Reduced assembly line time
- Improved assembly ergonomics
- Improved fuel economy via reduced weight
- Improved aerodynamic drag via reduced frontal profile OR
- Improved interior headroom for the same frontal profile
- Increased styling flexibility (assuming use of composites materials)

There of course exist disadvantages with a switch to new methods of construction and materials. While it has not been addressed within the current work thus far, one cannot discuss sandwich constructions without discussing composite materials such as fibre reinforced plastics. The discussion surrounding the advantages of composite materials in the automotive industry, especially with structural application in mind, has existed at least since the mid 1980's. With the exception of extreme applications such as supercars, there exist few current examples of composite sandwich structures making a significant contribution to a series production automobile. Previously, engineers have reduced vehicle weight by changing from standard grades of carbon steel to aluminium, magnesium, or high-strength stainless steel alloys. While this has been effective to a degree, vehicle curb

weights continue to rise and the choice of light weight metallic materials is dwindling if not already exhausted.

Presumably, the two greatest hinders to engineered materials in the automotive industry are cost and crash safety. Sandwich structures, especially those using fibre reinforced plastics are significantly more expensive to produce than their stamped steel equivalents using current methods of construction. It is however a fact that tooling required to produce a stamped steel structure is incredibly expensive, and production of such components must continue for several years to achieve a return on investment. Tooling required for composite based sandwich structures is a fraction of the cost, which would allow increased flexibility in design changes under a vehicle models lifetime; this must of course be balanced with the need for increased numbers of production stations to obtain the production rates necessary to maintain the existing assembly line speed. Certain methods of construction, for example the use of thermoplastics as face sheets and core material show promise, and increase both the speed at which components can be produced as well as the recycleability of the components.

With regard to crash safety, it is most certainly possible to create a vehicle using composite materials and sandwich construction that is as safe or safer than a stamped steel construction. The problem is of course not making the vehicle safe, but making it safe for a reasonable cost. Computational crash calculations take up the majority of CPU time in modern vehicle design and are the foundation of the vehicle design process. The current state of the art regarding the capacity to model, predict, and optimize the collapse of sandwich structures is vastly inferior to the level of understanding regarding metallic structures. Research in this are is ongoing and while it is likely only a question of time until the same level of reliability is reached in predicting crash behaviour of sandwich structures and composite materials as exists for metallic structures today, the question of how long it will take remains open. Unfortunately, the intermittent period between now and then would rely significantly on prototype crash tests, which are both expensive and time consuming, and at present reserved mostly for validation of numerical results.

One interesting aspect to the entire problem is the capacity of the automotive industry to find solutions for new and difficult problems. If the automotive industry as a whole should decide to embrace the technology and put its collective resources behind finding solutions, it will, without a doubt, shorten the process considerably. This however would require an investment in both time and financial resources that might not be favourably looked upon by the industry without significantly more stringent regulatory legislation.

One might be prone to think that, given the current focus on environmental issues and exhaust emissions as well as the more recent economic problems facing the global automotive industry, that a switch to methods which will could potentially save resources both economically and ecologically is lying "right around the corner". As the viewpoint of "right around the corner" has been re-iterated for nearly twenty five years, the question of how long the corner is, or if perhaps the corner is actually a roundabout remains to be answered.

6 Future Work

The work within this thesis has focused on the mass optimization of a sandwich panel to a given set of structural constraints. Acoustic properties have been assessed, but have been a passive component in the calculations. In future work, it is the intention of the author to implement a more complex multi-objective optimization problem where acoustic aspects as well as structural aspects will be active parts of the optimization. Additional design variables which will affect both the acoustic and structural properties of the structure shall be included such as material properties of the structural and acoustic foams, and mechanical properties of the face sheet materials.

Within the remaining time in this project, it is also hoped that the ecological and economical aspects of the optimization process can be assessed by more direct methods, such as perhaps life cycle analysis, or some kind of environmental impact factor.

Bibliography

[1] Oxford University Press, "The oxford english dictionary, second edition," 1989.

[2] Ford Motor Company, "http://www.ford.com/about-ford/news-announcements/featured-stories/featured-stories-detail/ford-modelt," Retrieved Feb 2009.

[3] J. Dargay, D. Gately, and M. Sommer, "Vehicle ownership and income growth worldwide:1960-2030," *The Energy Journal*, vol. 28, no. 4, pp. 143–170, 2007.

[4] The Saab Museum, "www.saabmuseum.com," Retrieved Nov 2008.

[5] www.carfolio.com, Retrieved Nov 2008.

[6] United Nations Framework Convention on Climate Change, "http://unfccc.int/," Retreived Jan. 2009.

[7] The Nobel Foundation, "http://nobelprize.org/nobel_prizes/peace/laureates/2007/index.htm/," Retrieved Jan 2009.

[8] United Nations Economic Commission for Europe, "Unece vehicle regulations no. 51-noise of vehicles having at least four wheels."

[9] D. Västfjäll, M.-A. Gulbol, M. Kleiner, and T. Gärling, "Affective evaluations of and reactions to exterior and interior vehicle auditory quality," *Journal of Sound and Vibration*, vol. 255, no. 3, pp. 501–518, 2002.

[10] K. Genuit and A. Fiebig, "The influence of combined environmental stimuli on the evaluation of acoustical comfort:case studies carried out in an interactive simulation environment," *Int.J.Vehicle Noise and Vibration*, vol. 3, no. 2, pp. 119–129, 2007.

[11] A. Miśkiewicz and T. Letowski, "Psychoacoustics in the automotive industry," *Acustica -acta acustica*, vol. 85, pp. 646–649, 1999.

[12] M.J.M.Nor, M.H.F.Fouladi, H.Nahvi, and A.K.Ariffin, "Index for vehicle acoustical comfort inside a passenger car," *Applied Acoustics*, vol. 69, pp. 343–353, 2008.

[13] M. Harrison, *Vehicle Refinement Controlling Noise and Vibration in Road Vehicles*. Elsevier Butterworth-Heinemann, 2004.

[14] N.Lalor and H.-H. Priebsh, "The prediction of low- and mid-frequency internal road vehicle noise: a literature survey," *Proc. IMechE, Part D:J.Automobile Engineering*, vol. 221, pp. 245–269, 2007.

[15] K. M. Lilley and P. E. Weber, "Vehicle acoustic solutions," *Sound and Vibration*, pp. 16–19, July 2003.

[16] R. F. Freymann, "Advanced numerical and experimental methods in the field of vehicle structural-acoustics," 2000. ISBN:3-89791-172-8.

[17] S.-H. Oh, H.-S. Kim, and Y. Park, "Active control of road booming noise in automotive interiors," *Journal of the Acoustical Society of America*, vol. 111, pp. 180–188, Jan 2002.

[18] F. Fahy, *Sound and Structural Vibration*. Academic Press, 1985.

[19] S.M.Beane, M.M.Marchi, and D.S.Snyder, "Utilizing optimized panel damping treatments to improve powertrain induced nvh and sound quality," *Applied Acoustics*, vol. 45, no. 2, pp. 181–187, 1995.

[20] M. D. Rao, "Recent applications of viscoelastic damping for noise control in automobiles and commercial aeroplanes," *Journal of Sound and Vibration*, vol. 262, pp. 457–474, May 2003.

[21] J.Bienert, "Optimisation of damping layers in car bodies," *Proceedings of the 2002 International Conference on Noise and Vibration Engineering, ISMA*, pp. 2005–2010, Sept 2002.

[22] D. Roesems, "A new methodology to support an optimized nvh engineering process," *Sound and Vibration*, pp. 36–45, May 1997.

[23] S. Subramanian, R. Surampudi, K. Thomson, and S. Vallurupalli, "Optimization of damping treatments for structure borne noise reduction," *Sound and Vibration*, vol. 38, pp. 14–18, Sept 2004.

[24] D. A. Wagner, Y. Gur, S. M. Ward, and M. A. Samus, "Modeling foam damping materials in automotive structures," *Journal of Engineering Materials and Technology*, vol. 119, pp. 279–283, 1997.

[25] M. Donley, W. Stokes, G. S. Jeong, J. K. Suh, and S. G. Jung, "Validation of finite element models for noise/vibration/harshness simulation," *Sound and Vibration*, pp. 18–23, August 1996.

[26] A. Kropp and F. Ihlenburg, "Influence of local damping on the acoustic design of passenger car bodies," *AutoTechnology*, vol. 4, pp. 60–63, Aug 2004.

[27] P. Davidsson, *Structure-Acoustic Analysis; finite element modelling and reduction methods*. PhD thesis, Lund University, 2004.

[28] UGS Corporation, *NX Nastran Quick Reference Guide*, 2007.

[29] UGS Corporation, *NX Nastran Advanded Dynamic Analysis Users Guide*, 2007.

[30] M.Carfagni, P.Citti, and M. Pierini, "Simplified finite element modelling of acoustically treated structures," *Journal of Sound and Vibration*, vol. 204, no. 5, pp. 705–716, 1997.

[31] M. S. Kompella and R. J. Bernard, "Variation of structural-acoustic characteristics of automotive vehicles," *Noise Control Engineering Journal*, vol. 44, no. 2, pp. 93–99, 1996.

[32] E. Hills, B.R.Mace, and N. Ferguson, "Acoustic response variability in automotive vehicles," *Journal of Sound and Vibration*, vol. 321, pp. 286–304, 2009.

[33] J.-F. Durand, C. Soize, and L. Gagliardini, "Structural-acoustic modeling of automotive vehicles in presence of uncertainties and experimental identification and validation," *Journal of the Acoustical Society of America*, vol. 124, no. 3, pp. 1513–1525, 2008.

[34] O. Gartmeier, "Noise and vibration in vehicle comfort design - a practitioners viewpoint - key note speech," in *Proceedings of ICSV 10*, (Stockholm, Sweden), 2003.

[35] J. Allard, *Propagation of Sound in Porous Media: Modelling Sound Absorbing Materials*. Elsevier Applied Science, New York, 1993.

[36] X.Sagartzazu, L. Hervella-Nieto, and J. Pagalday, "Review in sound absorbing materials," *Archives of Computational Methods in Engineering*, vol. 15, pp. 311–342, 2008.

[37] L. J. Gibson and M. F. Ashby, *Cellular Solids: Structure and Properties-Second edition*. Cambridge University Press, 1997.

[38] P.F.Soto, M. Herráez, A.González, and J. Saja, "Acoustic impedance and absorption coefficient measurements of porous materials used in the automotive industry," *Polymer Testing*, vol. 13, 1994.

[39] M.K.Ling, "Measurement of sound insulation of automotive body components using sound intensity," *Proc Instn Mech Engrs*, vol. 206, pp. 137–141, 1992. Technical Note.

[40] CDH AG, *Poroelastic material modelling and analysis with CDH\EXEL*, July 2007.

[41] N.-E. Hörlin, M. Nordström, and P. Göransson, "A 3-d hierarchical FE formulation of biot's equations for elasto-acoustic modelling of porous media," *Journal of Sound and Vibration*, vol. 245, no. 2, pp. 633–652, 2001.

[42] N.-E. Hörlin, "3d hierarchical hp-FEM applied to elasto-acoustic modelling of layered porous media," *Journal of Sound and Vibration*, vol. 285, no. 1-2, pp. 341 – 363, 2005.

[43] P. Göransson, "Tailored acoustic and vibrational damping in porous solids – engineering performance in aerospace applications," *Aerospace Science and Technology*, vol. 12, pp. 26–41, 2008.

[44] P. Göransson, "Acoustic and vibrational damping in porous solids," *Phil. Trans. R. Soc. A*, vol. 364, pp. 89–108, 2005.

[45] D. Zenkert, *An Introduction to Sandwich Construction*. Engineering Materials Advisory Services Ltd., EMAS, Solihull, UK, 1995.

[46] E. Bozhevolnaya and A. Lyckegaard, "Local effects at core junctions of sandwich structures under different types of loads," *Composite Structures*, vol. 73, pp. 24–32, 2006.

[47] A.F.Johnson and G.D.Sims, "Mechanical properties and design of sandwich materials," *Composites*, vol. 17, no. 4, pp. 321–328, 1986.

[48] G.S.Cole and A.M.Sherman, "Lightweight materials for automotive applications," *Materials Characterization*, vol. 35, pp. 3–9, 1995.

[49] National Highway Traffic Safety Administration, "Federal motor vehicle safety standard no. 208; occupant crash protection."

[50] National Highway Traffic Safety Administration, "Federal motor vehicle safety standard no. 214; side impact protection."

[51] National Highway Traffic Safety Administration, "Federal motor vehicle safety standard no. 216; roof crush resistance."

[52] G. Pitarresi, J. Carruthers, A. Robinson, G. Torre, J. Kenny, S. Ingleton, O. Velecela, and M. Found, "A comparative evaluation of crashworthy composite sandwich structures," *Composite Structures*, vol. 78, pp. 34–44, 2007.

[53] O. Skawinski, C. Binetruy, P. Krawczak, J. Grando, and E. Bonneau, "All-thermoplastic composite sandwich panels – part I : manufacturing and improvement of surface quality," *Journal of Sandwich Structures & Materials*, vol. 6, pp. 399–421, 2004.

[54] P. Feraboli, A. Masini, L. Taraborrelli, and A. Pivetti, "Integrated development of cfrp structures for a topless high performance vehicle," *Composite Structures*, vol. 78, pp. 495–506, 2007.

[55] S. G. Nash and A. Sofer, *Linear and Nonlinear Programming*. McGraw Hill, 1996.

[56] D.-C. Lee, H.-S. Choi, and C.-S. Han, "Design of automotive body structure using multicriteria optimization," *Structural and Multidisciplinary Optimization*, vol. 32, pp. 161–167, 2006.

[57] F. Duddeck, "Multidisciplinary optimization of car bodies," *Structural and Multidisciplinary Optimization*, vol. 35, pp. 375–389, 2008.

[58] J.Sobieszczanski-Sobieski and R.T.Haftka, "Multidisciplinary aerospace design optimization: survey of recent developments," *Structural Optimization*, vol. 14, pp. 1–23, 1997.

[59] S.Venkataraman and R.T.Haftka, "Structural optimization complexity: what has moore's law done for us?," *Structural and Multidisciplinary Optimization*, vol. 28, pp. 375–387, 2004.

[60] S.Kodiyalam, R.J.Yang, L. Gu, and C.-H.Tho, "Multidisciplinary design optimization of a vehicle system in a scalable high performance computing environment," *Structural and Multidisciplinary Optimization*, vol. 26, pp. 256–263, 2004.

[61] L. Gu and R.J.Yang, "On reliability-based optimisation methods for automobile structures," *Int.J.Materials and Product Technology*, vol. 25, no. 1/2/3, pp. 3–26, 2006.

[62] A. Kropp and D. Heiserer, "Efficient broadband vibro-acoustic analysis of passenger car bodies using an fe-based component mode synthesis approach," *Journal of Computational Acoustics*, vol. 11, no. 2, pp. 139–157, 2003.

[63] S. Marburg and H.-J. Hardtke, "A general concept for design modification of shell meshes in structural-acoustic optimization - part II: Application to a floor panel in sedan interior noise problems," *Finite Elements in Analysis and Design*, vol. 38, pp. 737–754, 2002.

[64] S. Marburg and H.-J. Hardtke, "Investigation and optimization of a spare wheel well to reduce vehicle interior noise," *Journal of Computational Acoustics*, vol. 11, no. 3, pp. 425–449, 2003.

[65] T.Yamamoto, S. Maruyama, S. Nishiwaki, and M. Yoshimura, "Topology design of multi-material soundproof structures including poroelastic media to minimize sound pressure levels," *Comput.Method Appl.Engrg.*, 2009. doi:10.1016/j.cma.2008.12.008.

[66] T.Fujii, S.Shibuya, Y.Sato, U.Jankowski, M.Müller-Bechtel, and P.Schneider, "New body in white concept through topology optimisation," *VDI-Berichte*, no. 1846, pp. 603–615, 2004.

[67] H. Mahmoud, P. T. Kabamba, A. Ulsoy, and D. G. A. Brusher, "Ranking subsystem targets according to their influence on system performance," in *Proceedings of the American Control Conference*, (Denver,Colorado), June 2003.

[68] N. S. Ermolaeva, M. B.G.Castro, and P. V. Kandachar, "Materials selection for an automotive structure by integrating structural optimization with environmental impact assessment," *Materials and Design*, vol. 25, pp. 689–698, 2004.

[69] K. Svanberg, "The method of moving asymptotes-a new method for structural optimization," *International Journal for Numerical Methods in Engineering*, vol. 24, pp. 359–373, Feb 1987.

[70] ASTM, "Astm d3039/d3039m standard test method for tensile properties of polymer matrix composite materials," tech. rep., 2000.

[71] J. Stoll and D. G. Schlotterbeck, "Headliners and other interior trim parts made of thermoformable urethane foam core sandwiches," *SAE Technical Paper Series*, vol. 900827, 1990.

[72] A.I.Soler and W.S.Hill, "Effective bending properties for stress analysis of rectangular tubesheets," *Transactions of the ASME: Journal of Engineering for Power*, pp. 365–370, July 1977.

[73] K.A.Burgemeister and C.H.Hansen, "Calculating resonance frequencies of perforated panels," *Journal of Sound and Vibration*, vol. 196, pp. 387–399, Oct 1996.

Division of work between authors

Paper A

Measurements were performed by Cameron with assistance from Saab and MWL Personnel. Post Processing of results was performed by Cameron. Nastran modelling was performed by Cameron and Hierarchical modelling by Göransson. Analysis and interpretation of results was jointly performed by Cameron and Göransson. Cameron wrote the paper with support from both Görransson and Wennhage.

Paper B

Modelling and analysis in Nastran was performed by Cameron. Cameron and Wennhage developed the optimization scheme together and Cameron executed it. Göransson provided the basis for the poro-elastic modelling. Cameron and Göransson implemented the acoustic analysis together. Cameron wrote the paper with support from Göransson , Wennhage and Rahmqvist.

Part II

Appended papers

Paper A

PREDICTION AND MEASUREMENT OF NOISE AND VIBRATION BEHAVIOR OF TRIMMED BODY COMPONENTS AT MID-FREQUENCIES

Christopher J. Cameron*, Per Wennhage, Peter Göransson

Centre for ECO^2 Vehicle Design
KTH Aeronautical and Vehicle Engineering,
Kungliga Tekniska Högskolan (KTH)
SE-100 44 STOCKHOLM, SWEDEN
http://www. eco2vehicledesign. kth. se

Abstract

The work within this paper focuses on the application and validation of numerical methods for predicting the acoustic and structural NVH behaviour of trimmed body components in an automotive context.

Specifically, the roof structure of a passenger car was investigated from various performance aspects, using both structural and acoustic excitation. The roof was initially tested in situ, with and without interior lining, to provide a reference for subsequent component tests. It was then detached from the car, mounted in a rigid frame and tested in a transmission window using both acoustic and structural excitation.

A finite element model of the detached component was developed using shell and solid elements for the structure and solid elements for the interior lining. Predictions were carried out to evaluate the sound transmission loss as well as the vibrational frequency response due to a force applied to the structure. Special attention was given to the modelling of the headliner as well as the air gap separating the headliner from the outer sheet metal.

The main objective of the current work has been to establish a datum reference for alternative designs. From this aspect, the validation of the numerical modeling methodology used was a crucial step. It was found that the predictions agreed very well with the measured data. As an additional, very interesting result, it was also found that the in-situ testing correlated well with the transmission suite testing.

Key words: acoustics, structural, equivalent, transmission, structure borne, interior trim, numerical modelling, measurement

1. Introduction

The importance of the noise and vibration (NVH) function requirements of modern vehicles are of ever increasing importance for vehicle manufacturers, perhaps even more emphasised with

*Corresponding Author
Email address: cjca@kth.se (Christopher J. Cameron)

the current trend towards environmentally compatible hybrid-electric power train concepts.

While the structural design of an automobile body during the last decades have come to rely heavily on finite element analysis, the NVH design traditionally has been based on the use of experimental prototypes and the skills of experienced engineers to adjust the acoustic properties of the full vehicle. For this purpose body treatments and interior trim components are added to provide aesthetics, thermal insulation and to control transmission of noise and vibration in order to improve the acoustic environment.

The vehicles acoustic interior trim has rarely been modelled in detail, if at all in industrial practice, and its effects are often accounted for by the use of global fluid damping constants and additional masses etc. The reason for these simplifications are several, both related to a fundamental lack of proper modeling methodology but also to computational efficacy, e.g. performing coupled fluid-structure analysis, including the effects of damping provided by the car interior, has in any given commercial code been computationally expensive, and furthermore usually limited to the frequency domain below 200Hz.

Thus there has been a need for improved simulation and modeling techniques, in order to allow better control of the early stages of the acoustic design of the full vehicle. Much research has been spent on this aspect during the last decades and different methods for predicting the acoustic properties of the full vehicle have been developed[1]. With the increase in computer power seen during the last decades, and the advancement in CAE/CAD tools, modelling of interior trim using finite element models has reached a level of maturity sufficient for industrial application.

The influence of the interior trimming is a crucial aspect of a full vehicle NVH simulation model, in particular concerning the often discussed medium frequency range, here somewhat arbitrarily defined as the frequency range between 100 and 500 Hz. As a vast majority of vehicle development work is done using computational methods, any new tools developed should be complementary to finite element analysis.

The work within this paper focusses on such methods for prediction of NVH behavior of trimmed body panels subjected to structural and fluid borne acoustic excitation. It is demonstrated that modelling of interior components, both for airborne and structure borne transmission can be used to investigate the effects of interior trim on the interior response. In particular, this study aims at investigating the interaction between the roof structure and the interior headliner trim component, and the sensitivity of this system to variations in roof liner properties and attachment conditions.

Measurements were made using a complete vehicle provided by Saab Automobile AB(SAAB). After removing the roof system, component tests were performed at the Markus Wallenberg Laboratory for sound and vibration research (MWL) at KTH to gain a better understanding of the roof components. Finally, a finite element model of the roof system including the acoustic trim was developed which can be used to study the interaction between the roof trim and the air cavities of the passenger compartment and the roof.

2. Method

Full vehicle acoustic measurements were performed in a semi-anechoic chamber at SAAB. Sound Transmission loss was measured according to international standardised methods [2, 3] both with and without the inner headliner installed.

The roof structure was removed from the vehicle and measured at MWL. Sound transmission loss testing was performed in addition to vibro-mechanical testing.

Tensile testing was performed to obtain the mechanical properties of the constituent components of the headliner. An equivalent solid representation was developed for the headliner to simplify the modelling using basic sandwich theory [4] and measured mechanical data.

Two different FE codes were used to simulate the acoustic behavior of the roof structure with the headliner as measured at MWL. Both codes use the equivalent solid representation of the headliner component. In house hierarchical FE code was used to calculate the sound transmission loss of the system using a geometrically simplified model. Vibro-mechanical analysis was performed using NX nastran 6.0. A model of the roof structure was created from an existing full vehicle model provided by SAAB. The interior headliner was modelled as a three dimensional solid, impervious to fluid flow. Acoustic damping within the Nastran model was achieved by the use of a surface impedance calculated according to the methods described in [5] and applied on the interior side of the headliner.

A direct comparison of the sound transmission loss for the full vehicle, component, and computational model across the mid-frequency range was performed.

A comparison of average vibrational velocities of measurement points in the laboratory and the numerical model was performed for both the outer roof sheet metal and the inner headliner. A parameter study was performed varying headliner stiffness, headliner fixation, surface impedance at the headliner, and the acoustic properties of the passenger cavity.

2.0.1. Full Vehicle Testing

Full vehicle testing was performed in the NVH laboratory at SAAB, in Trollhättan, Sweden. A semi-anechoic room with absorbent walls and ceiling and a hard floor was used for measurement. A standard production SAAB 9-3 Sport combi was supplied for the testing.

The vehicle was parked in the middle of the anechoic room and a 100W sound source was placed inside the vehicles passenger compartment. The source was supplied with a signal from a Brüel & Kjær Type 1405 white noise generator in the frequency range 250Hz -10kHz. A Brüel & Kjær Type 2706 power amplifier was used between the noise generator and the sound source.

Sound pressure within the vehicle was measured using 3 randomly placed pressure microphones moved to 24 different locations during the course of testing. Microphones were isolated from structural vibration by means of elastic cording.

Sound transmission loss for the roof system was measured by scanning the roof using a Brüel & Kjær Type 4135 two microphone sound intensity probe according to international standards[2].

Size constraints prohibited scanning of the entire roof in a single pass, and so it was broken up into 9 subsections. Subsections 1–7 were drawn out based on the location of cross-beams and additional structure under the outer sheet metal. Subsections 8 & 9 are the central and perimeter sections of the roof panel. Each subsection was scanned individually. Figure 1 shows a schematic of the subsection layout for scanning.

In total, the entire roof was scanned four times. The first complete scan consisted of sections 1–7. The second complete scan consisted of sections 8 & 9. This redundant scanning was done in order to see the effect of sound leakage through door and window seals–i. e. flanking transmission. The same measurements were performed after removing the inner headliner. This was done to measure the acoustic contribution of the headliner on the full vehicle scale.

Sound intensity for each subsection was measured and the Sound Reduction Index(SRI) for each section was calculated according to international standards [3]. SRI for the entire roof was calculated using the area weighted average of the subsection values. Values of the sound reduction index were plotted across the frequency spectrum and can be seen in the results section.

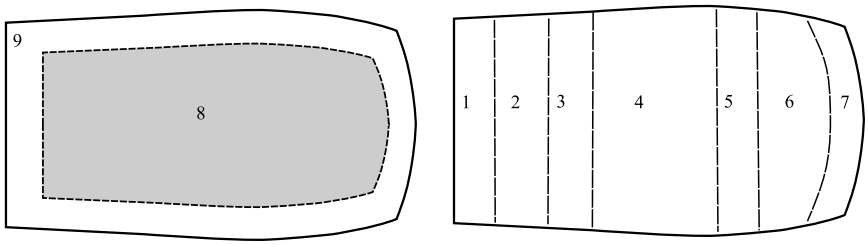

Figure 1: Area layout for sound intensity scanning measurement

2.0.2. Component Transmission Testing

After full vehicle testing, the roof section was removed from the car and attached to a rigid steel frame. All windows were removed and the openings were closed with MDF (fibre-board) panels and a layer of mineral wool, see figure 2. Silicone glue was used around the perimeter of the MDF panels to effectively seal the holes in an effort to eliminate any potential flanking transmission.

Figure 2: Roof Structure attached to steel frame with mdf closures

The structure was mounted between the reverberant and anechoic rooms at MWL. Due to the size of the roof and attached framework, the exterior surface of the roof faced the reverberant room and the headliner the anechoic room. A Brüel & Kjær Type 1405 signal generator was used to produce a white noise signal between 100Hz-5khz fed through an NAD C370 stereo integrated amplifier to a sound source in the reverberant room. Average sound pressure levels in the reverberant room were measured using a microphone mounted on a rotating boom. The measurement areas on the outside of the roof were re-drawn on the interior side of the headliner as accurately as possible. Sound intensity scanning was performed on the headliner side of the roof structure according to international standards [3]. It should be emphasised that the source and measurement sides of the roof as mounted in MWL are switched compared to the setup at SAAB. Figure 3 shows the roof as mounted in MWL for testing.

For the experimental setup at MWL, it was possible to measure the entire inner roof at once in

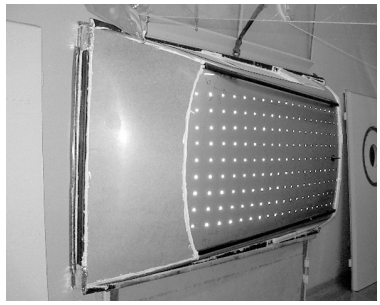

Figure 3: Roof Structure mounted in MWL

addition to the individual subsections. This enables SRI to be measured directly rather calculated as a sum of weighted averages. Results for SRI were plotted against the frequency interval and can be found in the results section.

2.1. Vibro-Mechanical Testing

In addition to the sound absorption capabilities of the roof structure, it was decided to characterise the structures response to mechanical vibration. Such a test provides both an important picture of the vibroacoustic properties of the component as well as a part of the experimental correlation. A Brüel & Kjær Type 1405 signal generator and Type 2706 power amplifier were used to excite a Brüel & Kjær Type 4809 inertia shaker attached to the structure at the midpoint of the driver's side A-Pillar. A threaded washer was glued to the A-pillar and a force transducer was screwed into to the washer. The shaker was suspended from a steel frame with rubber straps. A small diameter stinger was used to attach the shaker to the force transducer. Using a small diameter stringer ensured that the force applied to the structure was as close as possible to perpendicular to the sheet metal at the point of excitation.

A Brüel & Kjær Type 2635 charge amplifier was used to amplify the signal from the force transducer. A laser vibrometer consisting of a Polytec OFV 303 Sensor Head and Polytec OFV 3001 Controller was used to measure the vibration levels of the outer roof and the headliner. Reflective tape was used to mark the measurement points and enhance the reflected signal to the laser. Analysis of the signals was performed using siglab on a PC. The inertia shaker setup and the inner and outer roof measurement points can be seen in figure 4.

Vibrational velocity was recorded for 180 points on the exterior of the roof and 21 points on the interior side of the headliner. Matlab was used to post-process the data. Average vibrational velocity for the measured surface was calculated using the individual measurement points for the respective surface.

2.2. Tensile Testing of Headliner Components

The inner headliner is a sandwich construction consisting of two stiff fibre reinforced membranes separated by a foam core. On the interior side of the sandwich is a second layer of relatively soft open celled foam and a final layer of perforated fabric are used to provide sound absorption and an aesthetically appealing surface. Materials such as glass fibre reinforced plastics

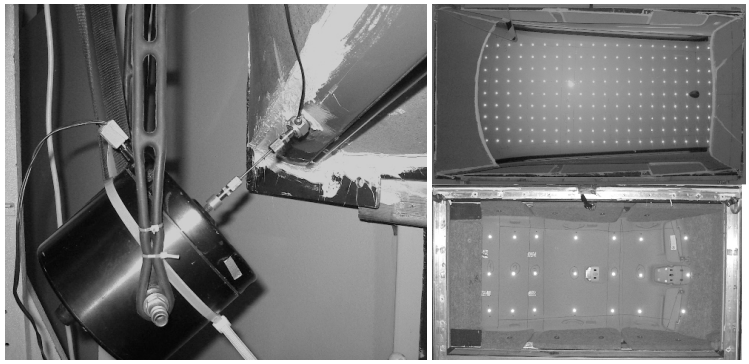

Figure 4: Inertia Shaker Attachment and Measurement Grid Points

and polyurethane foam are often used in headliner applications [10, 11] and while representative values can be obtained from the literature [7, 8] experimental testing was deemed necessary to obtain actual mechanical properties. Figure 5 shows a cross-section of the measured headliner.

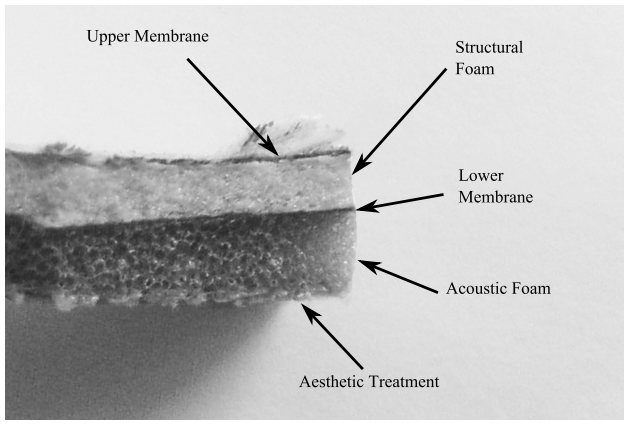

Figure 5: Cross-section of Headliner Construction

A square approximately 35cm by 35cm was removed from the centre section of the headliner. This area corresponds to the thickest and most uniform thickness part of the headliner. The upper membrane and lower membrane were peeled from the urethane foam core. Additionally, the soft inner foam layer was peeled from the inner membrane. Each layer was trimmed to a square 25cm x25cm. The urethane foam was weighed and its density calculated assuming a uniform thickness of 6.0 mm.

Tensile testing was performed according to ASTM standards [6]. This test method was used because the inner and outer membranes were of a glass fibre reinforced construction. Tabs for clamping, as described in the testing standard were not used as they were not deemed necessary to gain basic stiffness information. The same testing method was used for testing the foam samples. While the choice of this test method for the foam samples was not optimal, it was deemed accurate enough to gain an estimate of the foams properties.

Ten samples measuring 25mm by 250mm were cut from the outer membrane, urethane foam, and inner membrane respectively. Samples were placed in pneumatic clamps fitted to an Instron screw driven Universal Testing Machine. An extensometer and a 30kN load cell were used to record the load v/s displacement behavior of the samples. The extensometer was attached to the sample using rubber bands. A picture of the sample in the test rig can be seen in figure 6. Displacement control was used to regulate the rate of loading of the specimens.

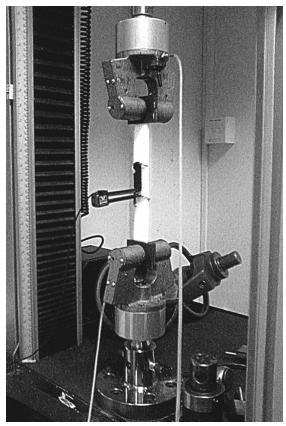

Figure 6: Tensile testing of headliner components

Stress v/s Strain plots were obtained by post processing the test results using Matlab(^{TM}). Within the initial elastic region of the deformation, a first order polynomial curve was fitted to the data to achieve a value for the Young's modulus. This was repeated for each of the test specimens, and average values for all the samples of a given component were calculated. For the fibre reinforced layers, a tensile Young's modulus of 9.1 GPa for the outer membrane and 4.8 GPa for the inner membrane was obtained. A tensile modulus of 8.8 MPa was obtained in the same manner for the urethane foam.

According to the literature, for a glass fibre reinforced phenolic composite, values of Young's modulus range from 4.5 - 7.5 GPa, depending upon whether the fibres are continuous or chopped [7]. This agrees well with test data for the inner and outer membranes, however it implies that some additional form of reinforcement is likely present in the outer membrane.

For the urethane foam, a density of 55.7 kg/m^3 was obtained. According to [8] the relationship between the polymeric solid and its corresponding open celled foam can be described as in Equation (1).

$$\frac{E_{foam}}{E_{solid}} \approx \left(\frac{\rho^{foam}}{\rho^{solid}}\right)^2 \tag{1}$$

Using the relationship in Equation (1) for the density calculated from the sample and using properties for solid polyurethane found in [8], yields a Young's modulus for the foam of 3.45 MPa. A compressive modulus of 10MPa is listed in [7] for a polyurethane foam of slightly lower density (30kg/m^3). This data would seem to indicate a somewhat exaggerated estimate of the urethane foams properties achieved by tensile testing.

2.3. Numerical Simulation

While some work has been done in analysing the effects of the roof cavity-headliner interaction [9] its effect is not well understood and seldom modelled numerically. The majority of information available regarding the acoustic or structural properties of headliners comes from the headliner manufacturers themselves [10, 11]. A method for numerically analysing the acoustic properties of the acoustic trim would be an interesting step towards an independent in-situ design methodology.

2.3.1. Modelling of the Headliner

Accurate modelling of each individual layers of the headliner as shown in figure 5 would be computationally quite expensive due to the small thicknesses and necessity for a great number of elements. A modelling approach more suitable to an industrial environment was desired, and so another method of modelling the headliner was developed where a homogeneous three dimensional element with isotropic properties could be used instead.

The upper three layers within the headliner make up a classical sandwich structure. The stiffness contribution of the aesthetic fabric treatment and the soft, porous acoustic foam to the overall stiffness of the headliner can be ignored. For a sandwich structure, the Young's modulus through the thickness varies depending on the material layer. Figure 7 shows the cross-section for an arbitrary sandwich with dissimilar faces.

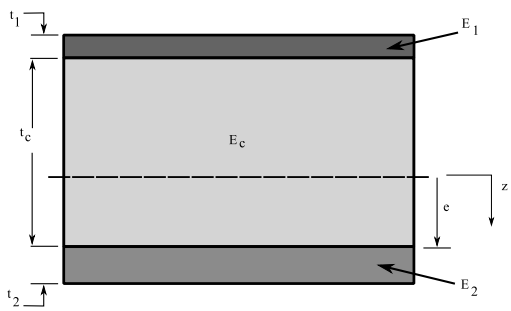

Figure 7: Arbitrary sandwich cross-section (Redrawn from [4]

The flexural rigidity of a sandwich beam describes the structures stiffness in bending. Flexural rigidity for a unit width sandwich beam, denoted as D, of arbitrary cross section as shown in figure 7 can be expressed in the following manner [4]:

$$D = \int Ez^2 dz = \frac{E_1 t_1^3}{12} + \frac{E_2 t_2^3}{12} + \frac{E_c t_c^3}{12} + E_1 t_1 (d-e)^2 + E_2 t_2 (e)^2 + E_c t_c (\frac{t_c + t_2}{2} - e)^2 \quad (2)$$

Where:

$$e = \frac{E_1 t_1 d}{E_1 t_1 + E_2 t_2} \quad (3)$$

$$d - e = \frac{E_2 t_2 d}{E_1 t_1 + E_2 t_2} \quad (4)$$

$$d = \frac{t_1}{2} + t_c + \frac{t_2}{2} \quad (5)$$

Lower case t denotes a thickness, and E is the Young's modulus. Subscripts 1 and 2 denote the upper and lower face sheets. Subscript c denotes the core material. In this case, the face materials are the two fibre reinforced membranes and the core the polyurethane foam layer. Lower case z denotes the vertical coordinate of the sandwich cross-section where $z = 0$ is the neutral axis of the sandwich structure. By inserting values of t and E into Equation (2), a value can be obtained for the flexural rigidity.

21 square samples were cut from the headliner at the measurement points of the inner roof and the thickness for each of the layers were measured. A range of thicknesses was found to exist within the upper structural foam layer, most likely due to the manufacturing process which often involves pressing[10]. Thicknesses of the membranes, inner foam layer, and porous fabric layer were constant. The thickness of the urethane foam varied from 1.5 mm to 6.0 mm. A nominal thickness of 4.0 mm was chosen to use in the FE model. The inner foam/fabric layer was constant at 2.0 mm.

A total nominal thickness for the entire headliner in the model was chosen as 6.0 mm. Two layers of hexagonal solid elements were used to model the headliner following the geometry of the inner surface. Holes for attachment of lighting, etc., were ignored.

Using the calculated values of flexural rigidity, together with the fixed mesh thickness of 6.0 mm, an equivalent value of Young's modulus for the solid can be obtained by manipulating Equation (2) so that E_{equiv} can be calculated as follows:

$$E_{equivalent} = \frac{D}{\int z^2 dz} = \frac{D}{\frac{(6.0)^3}{3}} [MPa] \quad (6)$$

Using this method, a range of values for E_{equiv} was obtained. A minimum equivalent stiffness of 101.0 MPa and a maximum equivalent stiffness of 1358.8 MPa were obtained. A nominal value of E_{equiv} for an estimated average core thickness of 4.0 mm and measured stiffness for each of the various layers was calculated to 622.0 MPa.

Due to the constantly changing cross-section thickness and uncertainty in exact material properties, it was not deemed sufficiently accurate to calculate the equivalent density based on the material properties and geometry. Instead, an equivalent density was calculated by using the actual mass of the headliner and the volume of the headliner model according to:

$$\rho_{equivalent} = \frac{Mass_{actual}}{Volume_{model}} \quad (7)$$

In the vehicle, the headliner is equipped with wiring and lighting systems. This mass is accounted for within the equivalent density calculation. The local stiffness effects of these components were however ignored.

2.3.2. Numerical Sound Transmission Loss

Sound transmission loss was calculated using in-house hierarchical FE for poroelastic materials [12, 13, 14]. For these calculations, a geometrically simplified model was used. The model consisted of layers of simple rectangular boxes of representative size and thickness. The bottom layer was a fluid cavity of an equivalent size to that in the vehicle. This fluid cavity was attached to a layer representing the headliner. The headliner was in turn attached to a second much smaller air cavity representing the gap between the headliner and the roof sheet metal. Following this was a layer representing the sheet metal and finally a third layer of air.

Higher order polynomials (5th order up to 500 Hz and 8th order up to 1000 Hz) were used in order to permit accurate calculations without unnecessarily increasing the number of elements within the model.

Normal incident acoustic waves were used as an acoustic load through the frequency range of 100-500Hz. The simulation model was described in detail in [15] and will not be repeated here.

Sound transmission loss was then calculated in the same manner as performed with experimental measurements, but here using values from the numerical model. Incident and transmitted wave amplitudes were taken from the computed results and the transmission loss calculated.

2.3.3. Numerical Vibro-Mechanical Response and Parameter Study

Vibro-mechanical simulation was carried out using the commercial FE code NXNastran 6.0. A full vehicle FE model was provided by SAAB and modified to contain only the components in the structure seen in figure 2. The tubular steel frame which the roof structure was welded to, and shown in figure 2, was not included. The steel plates which the pillars were welded to were included in the model and used to apply boundary conditions. The edges nodes for the plates were restricted in all translational and rotational degrees of freedom. By applying such boundary conditions, it was assumed that the stiffness contributed of the tubular steel frame to the entire structure could be ignored.

Based on the assumption that the headliner is of such construction that fluid may not pass through, it becomes necessary to separates the passenger compartment into two fluid cavities. These two air volumes are herein referred to as the roof cavity and the passenger cavity respectively. The roof cavity is the air space between the inner headliner and the exterior sheet metal. The passenger cavity is the remaining fluid in the passenger compartment including the volumes within the doors. Within the vehicle, while fluid may not pass through the headliner, no airtight seal exists around its perimeter. To account for this the two fluid cavities within the model are connected via the enclosed airspace within the A, B, C, and D pillars. Figure 8 shows a cross-section of the complete FE model as implemented in Nastran.

2.3.4. Headliner Boundary Conditions

Attachment of the headliner to the structure of the vehicle is usually achieved by the use of plastic and metallic clips. The exact stiffness of these attachments was unclear in the present vehicle, and their actual influence on the performance of the trim component unknown, and so it was decided to investigate several scenarios numerically.

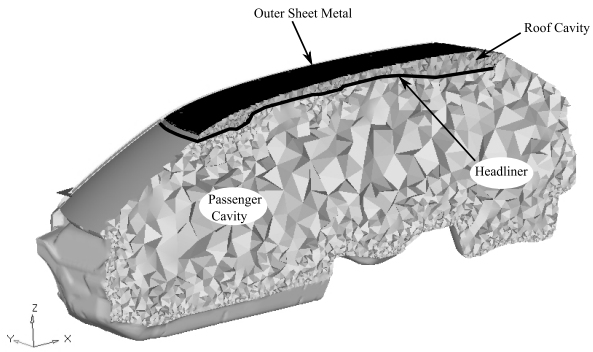

Figure 8: Cross-Section of FE Model

In the first configuration the clips are replaced by rigid elements between the attachment points on the headliner and the corresponding point on the structure. Nodes along the front and rear edge of the headliner are restricted in translational degrees of freedom as in the actual vehicle, the headliner is held in place using other trim components along these edges.

In a second configuration, the rigid body elements connecting the headliner to the structure are removed and the headliner is held in place by the boundary conditions along the front and rear edges of the headliner.

In the third configuration, the rigid body elements are present and the boundary conditions along the front and rear edges are removed.

2.3.5. Headliner Damping Properties

Ordinarily, damping within fluid-structure analysis in Nastran is obtained by using global structural and fluid damping factors $paramG$ and $ParamGFL$ respectively [16, 17]. In this model, the damping was achieved in a different method. Data from other laboratory measurements together with the models described in [5] were used to calculate numerical values for the frequency dependant surface impedance of the headliner.

In order to test the sensitivity of the model to the surface impedance of the headliner, calculations were performed with three different values. Values of 0.5, 1.0, and 2.0 times the nominal estimated surface impedance were used. Additionally, the surface impedance was removed completely to see its effect.

2.3.6. Effect of a Finite Cavity

During measurements, the interior side of the roof structure faced the anechoic room at MWL. This chamber represents an infinite cavity with zero reflection of sound waves at the walls. Within the numerical model, a finite cavity was used for the passenger compartment. It was desired to study the effects of this cavity on the vibrational vibrational response of the structure. Two variations on the nominal stiffness configuration were calculated. In one variant, a surface impedance was applied to all external surfaces of the passenger compartment acoustic cavity to simulate an infinite cavity. In the second variant, the passenger compartment acoustic

cavity was removed entirely. It was thought that external impedance configuration should reduce the impact of acoustic resonance modes within the cavity. In the second configuration, removing the cavity would completely eliminate any effects caused by acoustic modes of the passenger cavity, however the lack of coupling between the roof cavity and the passenger cavity may effect the resonant behavior of the roof cavity, and thus the structures vibrational response.

Direct frequency response analysis was carried out using NXNastran. A load of 50.0 N was applied at the mid point of the drivers side A-pillar. Frequency intervals of 5.0 Hz were used within the frequency range 100-500Hz. Fluid-structure coupling was performed using the advanced search method (AS) in NXNastran 6.0 and specifying restricting structural coupling to only the exterior roof panel and the interior lining. Structural response of the roof panel and the headliner was taken from the nodal values of velocity from nodes located as close to the measured points as possible.

3. Results

3.1. Sound Transmission Loss

Figure 9 shows the SRI calculated from laboratory measurements in 1/3 octave bands. All 9 measurement sections are included as well as the mean values for sections 1–7 and 8–9. It should be noted that while values of SRI for each subsection are included in figure 9, due to the relatively small area and short measuring time, these individual values should only be considered for reference purposes.

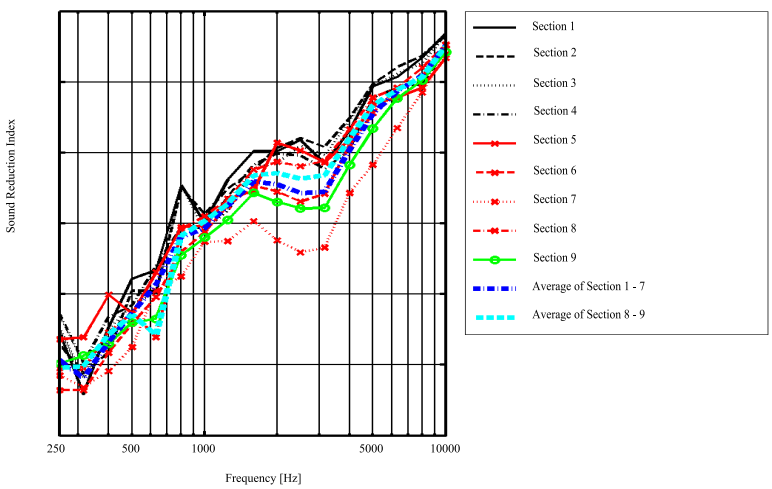

Figure 9: SRI values in 1/3 octave bands for roof subsections - Full vehicle with headliner

Figure 10 shows the directly measured SRI for the roof as tested in MWL in addition to the results from full vehicle testing at SAAB with and without the headliner.

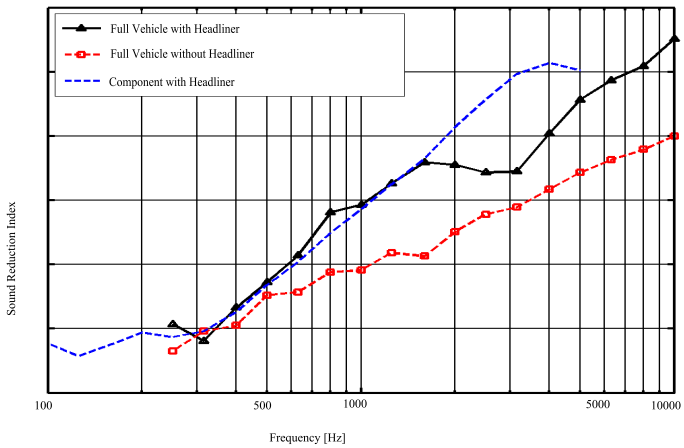

Figure 10: SRI in 1/3 octave bands - Full vehicle with and without headliner and component with headliner

Figure 11 shows the numerical values of STL as calculated with the hierarchical code together with the measured values.

3.2. Mechanical Vibration

Figures 12 through 21 show results for measured and numerical vibro-mechanical response of the inner headliner and outer roof as tested and in the configurations described in section 2.3.3 through section 2.3.6. All results are plotted using a dB scale on the vertical axis with 10 dB between the tick marks. A detailed explanation of these figures is left to section 4.2.

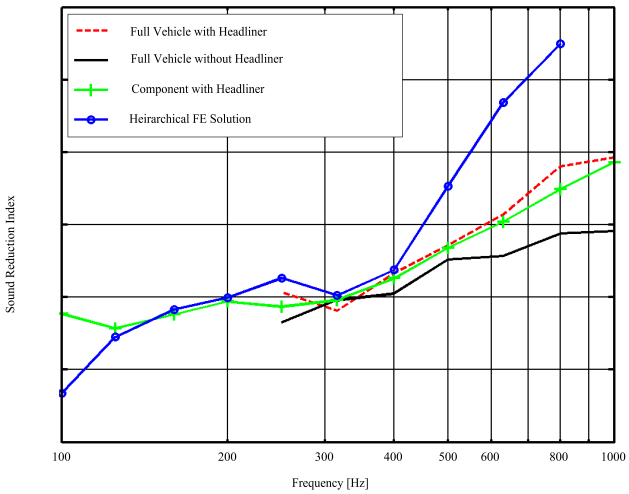

Figure 11: Measured and Numerical Sound Transmission Loss in 1/3 octave bands

4. Discussion

4.1. Sound Transmission Loss Measurement

In general, in figure 9, the trends for the individual sections agree with each other with the exception of a few measuring points. The largest deviation from the mean values occurs for subsection 8 in the region of 630 Hz, and subsection 7 from 1250 Hz and upwards. Lowered absorption for subsection 7 is most likely due to a combination of geometry and material configurations in the region. As subsection 7 lies along the front header beam, the double wall effect present in the rest of the roof is less dominant. This is also an area where a significant amount of interior details (lamps etc) are attached to the headliner. Section 7 is also adjacent to the windshield, which is less efficient at preventing sound transmission. A peak in absorption for sections 1, 2, and 3 at the 800 Hz measurement point can also be seen. This is most likely due to the geometry of the vehicle in that region. A transverse beam with attachment points for the rear tailgate takes up a significant amount of space in this region.

In figure 10 it can be seen that up to 1600 Hz, there is very good agreement between the full vehicle testing performed at SAAB and the laboratory testing performed at MWL. Above 1600 Hz there is significant deviation between the laboratory measurements and the mean value calculated from the full vehicle testing. While this may partially be caused by leakage through door seals etc, it is believed that the glass in the windshield and side windows may be a larger contributor. Glass has a reduced sound reduction index compared to the full roof structure in the frequency range in question. An indicator that sound leakage takes place can be seen in curve for subsection 8 in figure 9. Section 8 is measured further away from the glass surfaces, and any

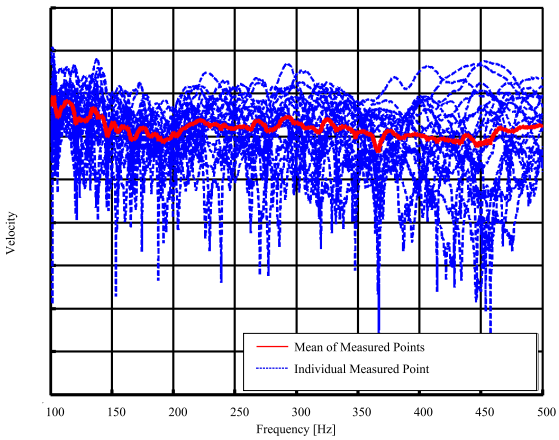

Figure 12: Measured Velocity Response of Headliner

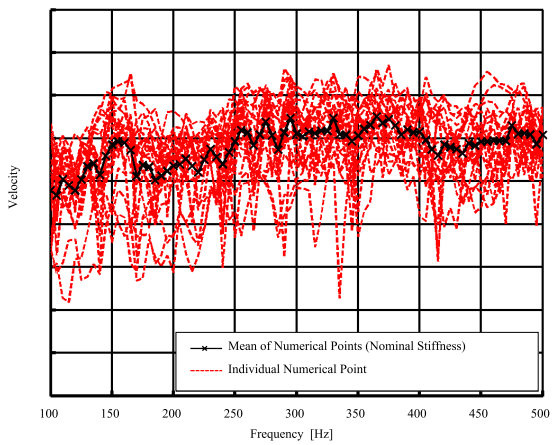

Figure 13: Numerical Velocity Response of Headliner with Nominal Stiffness Properties

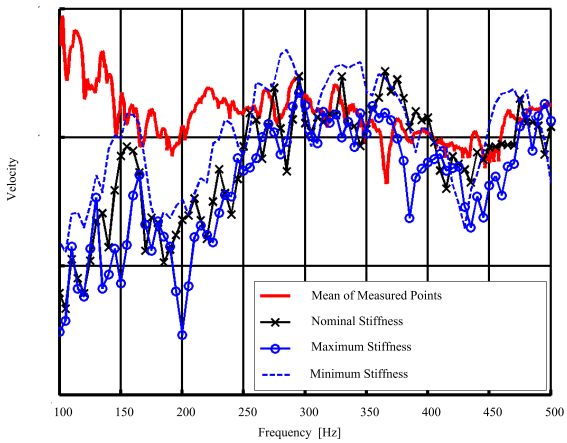

Figure 14: Measured & Numerical Velocity Response of Headliner including variations in Headliner Stiffness

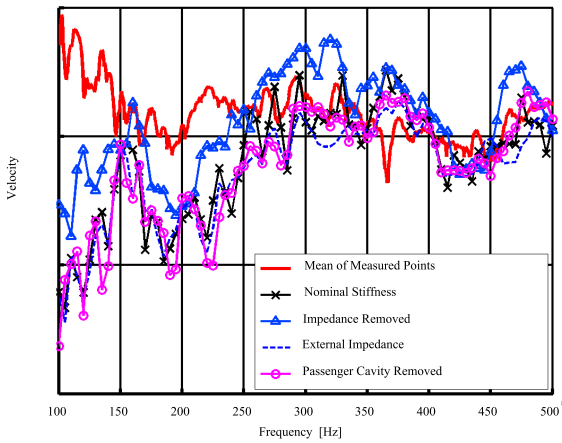

Figure 15: Headliner response with Impedance on exterior surfaces and passenger cavity removed

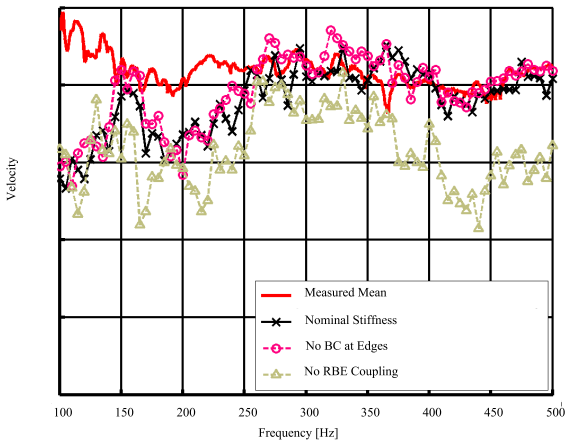

Figure 16: Headliner response with boundary conditions and rigid element coupling removed compared with nominal response and measure response

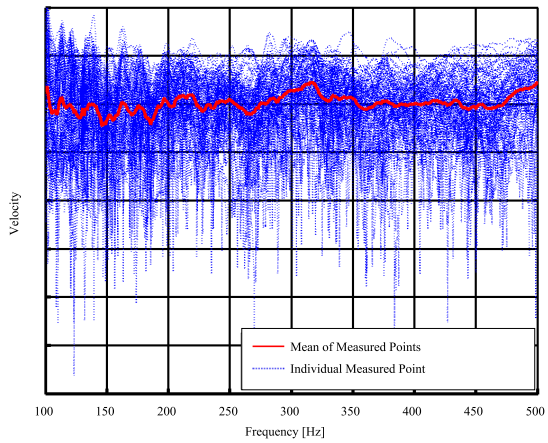

Figure 17: Measured Velocity Response of Outer Roof

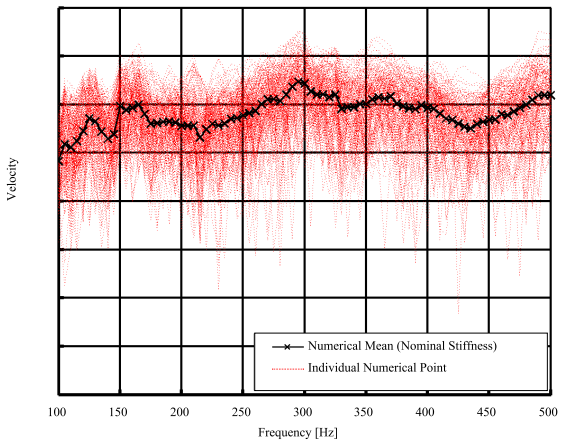

Figure 18: Numerical Velocity Response of Outer Roof

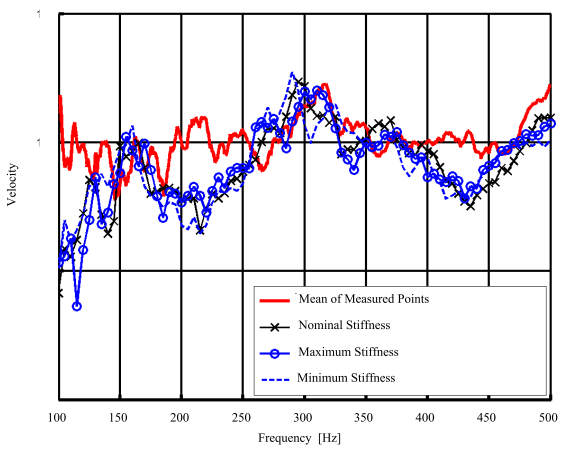

Figure 19: Measured & Numerical Velocity Response of Outer roof for variations in Headliner Stiffness

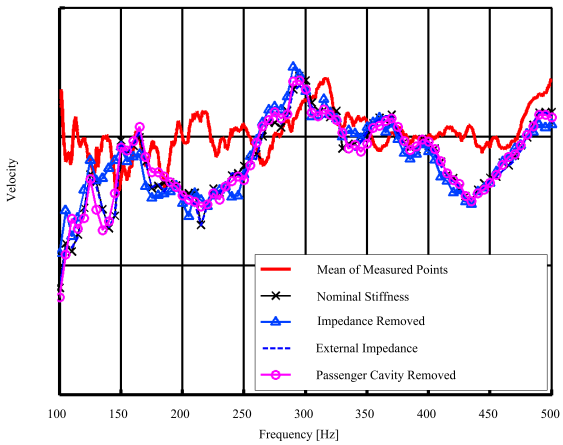

Figure 20: Outer roof response with Impedance on exterior surfaces and passenger cavity removed

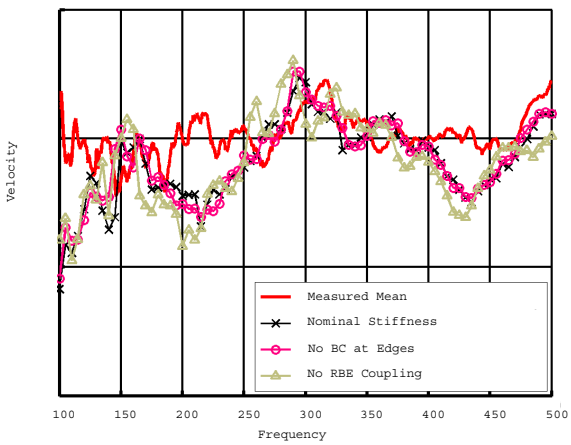

Figure 21: Outer roof vibrational response with variation of Headliner BC's

potential leakage sources, and shows a higher sound reduction index through the frequency range in question. For the laboratory case where the glass was removed and replaced with MDF and insulation, the curve does not deviate as in full vehicle testing. For reference purposes, the curve for sound reduction index without the inner roof panel as obtained at SAAB is also included. It is immediately obvious that the headliner construction contributes considerably to the sound transmission loss properties of the roof construction.

Figure 11 shows rather good agreement between the sound transmission loss calculated and the measured values up to about 500 Hz. Above this frequency the oblique incidence waves in the measured transmission loss become dominant. Since these are not present in the simplified model, the conclusion is that the simplified model provides sufficiently accurate sound transmission loss prediction for the full vehicle in the mid-frequency range.

4.2. Vibro-Acoustic Analysis

Figure 12 shows the measured frequency response functions of all 21 points measured on the inner roof together with the mean level of vibration across the frequency range of 100-500 Hz. Dashed lines show the measured values for individual points, and the solid line shows the average value. It can be seen that envelope in the measurements is more narrow for the lower frequency measurements and widens slightly in the higher frequencies. Maximum response in general stays within approximately 10 dB of the mean value. In the discussion of the sensitivity analysis below, the mean value of the vibration level will be used.

Figure 13 shows the numerical results for the inner roof for 21 points located at approximately the same location as in measurements. Direct frequency response was performed in 5.0 Hz steps between 100 and 500Hz.

Figure 14 shows the comparison of the measured mean vibration level and the numerical values for the nominal, high and low stiffness configurations as computed with Nastran. In general, rather good agreement can be seen through the majority of the frequency spectrum studied for all three stiffness configurations. Each stiffness configuration follows approximately the same trend with some slight variation. The results show that a reduction in stiffness leads to an increased vibrational velocity level and vice-versa. This behavior may be attributed to the coupling to the acoustic cavities. The stiffer the headliner, the less the impact of the acoustic pressure on the level of vibration. Below 250 Hz, the low stiffness configuration shows slightly better agreement to the measured results, however above 250Hz, the nominal configuration appears to better follow the measured curve.

Figure 15 shows the effects of the finite cavity and impedance on the results. Measured results and the nominal stiffness case are plotted for reference. In general, it can be seen that both removing the passenger cavity and applying an external impedance reduce the peek response of the headliner at localised maxima. This effect is most prevalent at the four nominal stiffness response peaks in the region from 250-300 Hz. Removal of the surface impedance at the headliner produces an increased level of vibration across the spectrum, exceeding measured levels for a large portion of the spectrum. Altering of the magnitude of impedance from 0.5 to 2.0 times the nominal value had almost no effect on the response compared to the nominal case and these results are therefore omitted.

Figure 16 shows the effect of boundary conditions and structural coupling on the headliner. In the case where the front and rear end boundary conditions have been removed, it can be seen that the curve follows quite well the case of nominal stiffness. Around 150 Hz, the case of removed boundary conditions shows better agreement with the measured values. Arguably, the

same is true above 400 Hz. For the case in which the RBE coupling has been removed, there is a very clear reduction in vibration levels, and a much poorer agreement between the calculations and measurement.

Figure 17 shows the measurement data for the outer roof of the structure. In total, 180 points were measured. Again, as for the case of the headliner, it can be seen that the envelope in the measurements is limited to approximately 10 dB around the mean.

Figure 18 shows the numerical simulation data for the outer roof panel wherein nominal headliner properties were used in the model.

Figure 19 shows a comparison of the measured mean vibration level and the numerical mean vibration level for the model using high, nominal, and low stiffness. For all three cases of stiffness, the general trend is quite similar and it is not obvious which, if any, has a larger effect on vibration level. Measured data and numerical data show very good agreement, with the exception of the region below 150 Hz. This maximum deviation is approximately 10 dB.

Figure 20 shows the effect of the passenger cavity and impedance variations on the outer roof's vibration level. There is a general good agreement between measurements and numerical results. While a small amount of variation does exist between the four numerical cases, the variation is relatively small. This would seem to indicate that for the external structure, the acoustic effects of the passenger cavity have little effect.

Figure 21 shows the effect of the headliner boundary conditions and attachment on the vibration level of the outer roof. While all three numerical solutions follow quite closely the same general trend, it is obvious that the rigid coupling between the headliner and the structure deviates the most from the measured data.

In the majority of the above mentioned figures, a rather good agreement between measurement data and numerical data has been found. Sources found in the literature [18, 19, 20] show that the difference between the numerical results and the measured data can lie well within the statistical spread for structural borne noise within larger populations of production vehicles. As only one vehicle was measured, this hypothesis cannot be tested.

An interesting trend can be noted by observing that both the numerical results for the headliner and outer roof exhibit a somewhat better agreement with the measured data at higher frequencies. An obvious explanation for this result is of course the difference in boundary conditions between tests and simulation.

Within the model, it has been assumed that all intersections between the pillars and the steel plates are welded completely. This is most likely not the case in the actual structure. Additionally, in the model it has been assumed that all edges of the steel plates are fixed. In the actual structure, the continuity of the welds may be questionable. Any discrepancy between the boundary conditions of the model compared to the laboratory will of course affect the agreement of results. This is emphasised for low frequencies.

Another large difference between the model and the measured structure is the acoustic environment. In MWL, the outer sheet metal was in contact with the air in the reverberation room, while the headliner was in contact with the fluid in the anechoic room. While some attempts to emulate the anechoic room were made, the effects of the reverberant room were not included.

Results have been presented for calculations using a wide range of properties for the inner headliner. As may be expected, the variations of stiffness, boundary conditions , and damping have a larger impact on the behavior of the headliner than on the outer roof. However, interestingly, a tenfold change in the stiffness of the headliner has marginal effect on its vibrational behavior. Reducing the effect of the passenger cavity also has little effect on the headliner's vibrational level.

One change that is significant is the removal of the rigid element coupling between the headliner and the steel structure. For both the case of the headliner vibration levels and the outer roof vibration levels, removal of the physical coupling between the two showed the most pronounced effect indicating a primarily structure borne transmission being dominant. It is perhaps not surprising that the removal of a coupling between two structures immersed in a fluid will have a significant effect in the systems vibrational behavior; however that this effect would be the most important effect regarding the properties of the headliner is significant.

Calculations with variations in impedance as described in section 2.3.5 showed almost no difference, varying only in the fifth or sixth decimal point and are therefore not included. This is in itself a quite interesting result, as it would indicate that the damping properties of the headliner do not have a significant effect on the mechanical response of the structure, so long as the damping is of an approximate magnitude.

The modelling of the headliner performed in this work was at a quite simplistic level and oversimplifications were no doubt made. Nevertheless, agreement between measurements and numerical models are quite good.

5. CONCLUSIONS

Sound transmission loss measurements have been performed on a full vehicle and on the component level. Very good agreement between results for both cases has been found. In certain frequency areas, glass windows are the most likely cause of reduced sound reduction capability for a trimmed body panel. Confirmation has been made of the significant contribution to sound transmission loss by the headliner in the vehicle. Results show that for trimmed body panels, in-situ measurement is sufficient for measuring the sound reduction index of the trimmed panel.

Numerical methods have also been used to estimate sound reduction index for trimmed body panels. These results show that geometrically simple models using hierarchical finite element code can give very accurate and reliable results for the sound reduction capability of trimmed body panels in the frequency range up to 500 Hz.

Vibro-mechanical testing of a roof structure has also been performed and the vibrational behavior of a roof headliner and outer roof panel have been measured. A finite element model was constructed with special consideration given to dividing the air cavity within the passenger compartment into two separate sections and including the headliner. The headliner was modelled using 3D elements and given equivalent homogeneous properties based on basic sandwich theory. Fluid damping was accomplished using surface normal impedance calculated based on the assumed construction of the headliner.

Very good agreement was achieved between the measured vibration levels and their numerical equivalents for both the headliner and outer roof panel.

Large changes in stiffness of the headliner have little effect on its vibrational behavior, as well as altering the damping properties of the headliner has almost no effect on the vibrational behavior of the system. Removing the damping completely does however affect the systems behavior.

Applying a surface impedance to the passenger acoustic cavity or removing it entirely from the model has a slight impact on the systems behavior, mostly in reducing peak vibrational responses due to the cavity. This would indicate that it is necessary to have the cavity present for predicting actual acoustic phenomena inside a production vehicle.

The coupling between the headliner and the structure was found to be the single most important factor of those studied. The presence or absence of a rigid coupling between the headliner and the surrounding structure has a significant effect on the system response.

The results also show that the material properties of the headliner are not important. As long as the headliner provides some sort of fluid damping of an approximate magnitude its specific construction is not a factor in its acoustic performance. Special attention should however be paid to the method by which the headliner is attached to its surrounding structure. In this model, rigid links were used as a simplification, however, based on the results of the simulations performed, it is likely that the stiffness of actual fasteners will impact on the behavior of the headliner and the surrounding structure.

Results of this work indicate that the standard practice of ignoring the vibro-mechanical impact of trim components within the vehicle may result in incorrect computational results. Two models have been developed to calculate the sound transmission loss and vibro-mechanical response of a trimmed body component, both of which show very good agreement with measured results. The accuracy of the modelling methods combined with the simplicity of their implementation would make them excellent candidates for industrial use, which would allow engineers to better understand the trim as an engineering component rather than a band-aid solution to a misunderstood acoustic phenomena within a finished vehicle.

6. ACKNOWLEDGEMENTS

This work was performed within the Centre for ECO^2 Vehicle Design with financial support from the Swedish Agency for Innovation Systems (VINNOVA), KTH, and Saab Automobile AB. The assistance of associate professor Leping Feng, KTH MWL, in the measurements performed is also acknowledged.

References

[1] N.Lalor and H-H Priebsh. The prediction of low- and mid-frequency internal road vehicle noise: a literature survey. *Proc. IMechE, Part D:J.Automobile Engineering*, 221:245–269, 2007.

[2] International Organization for Standardization(ISO). International standard 9614-2:1996 *Acoustics-Determination of sound power levels of noise sources using sound intensity- Part 2:Measurement by scanning*, 1996.

[3] Swedish Standards Institute. Swedish standard ss-en iso 15186-1 *Acoustics-Measurement of sound insulation in buildings and of building elements using sound intensity-Part 1:Laboratory Measurements(ISO 15186-1:2000)*, 2000.

[4] D. Zenkert. *An Introduction to Sandwich Construction*. Engineering Materials Advisory Services Ltd., EMAS, Solihull, UK, 1995.

[5] J.F. Allard. *Propagation of Sound in Porous Media: Modelling Sound Absorbing Materials*. Elsevier Applied Science, New York, 1993.

[6] ASTM. Astm d3039/d3039m standard test method for tensile properties of polymer matrix composite materials. Technical report, 2000.

[7] B.T.Åström. *Manufacturing of Polymer Composites*. Chapmann & Hall, 1997.

[8] L.J. Gibson and M.F. Ashby. *Cellular Solids: Structure and Properties-Second Addition*. Cambridge University Press, 1997.

[9] H.G. Choi, S.W. Kang, S.H. Lee, and J.M. Lee. A coupling analysis of interior noise of a vehicle with a roof-gap-trim effect. In *Proceedings of the 15 International Modal Analysis Converence-IMAC*, pages 444–449. SEM, Bethel, CT, USA, February 1997.

[10] J.R. Stoll and D.G. Schlotterbeck. Headliners and other interior trim parts made of thermoformable urethane foam core sandwiches. *SAE Technical Paper Series*, 900827, 1990.

[11] E. Haque. Designing strength, stiffness and acoustics in headliner substrate material. *Auto Technology*, 5:42–45, 2006.

[12] N.-E. Hörlin, M. Nordström, and P. Göransson. A 3-d hierarchical fe formulation of biot's equations for elasto-acoustic modelling of porous media. *Journal of Sound and Vibration*, 245(2):633–652, 2001.
[13] N.-E. Hörlin. 3d hierarchical hp-fem applied to elasto-acoustic modelling of layered porous media. *Journal of Sound and Vibration*, 285(1-2):341 – 363, 2005.
[14] P. Göransson. Tailored acoustic and vibrational damping in porous solids – engineering performance in aerospace applications. *Aerospace Science and Technology*, 12:26–41, 2008.
[15] P. Göransson. Acoustic and vibrational damping in porous solids. *Phil. Trans. R. Soc. A*, 364:89–108, 2005.
[16] UGS Corporation. *NX Nastran Quick Reference Guide*, 2007.
[17] UGS Corporation. *NX Nastran Advanded Dynamic Analysis Users Guide*, 2007.
[18] M.S. Kompella and R.J. Bernard. Variation of structural-acoustic characteristics of automotive vehicles. *Noise Control Engineering Journal*, 44(2):93–99, 1996.
[19] E.Hills, B.R.Mace, and N.S. Ferguson. Acoustic response variability in automotive vehicles. *Journal of Sound and Vibration*, 321:286–304, 2009.
[20] J.-F. Durand, C. Soize, and L. Gagliardini. Structural-acoustic modeling of automotive vehicles in presence of uncertainties and experimental identification and validation. *Journal of the Acoustical Society of America*, 124(3):1513–1525, 2008.

Paper B

STRUCTURAL-ACOUSTIC DESIGN OF A MULTI-FUNCTIONAL SANDWICH PANEL IN AN AUTOMOTIVE CONTEXT

Christopher J. Cameron[⋆], Per Wennhage[⋆], Peter Göransson[⋆] , Sven Rahmqvist[†]

[⋆]Centre for ECO^2 Vehicle Design
KTH Aeronautical and Vehicle Engineering,
Kungliga Tekniska Högskolan (KTH)
SE-100 44 STOCKHOLM, SWEDEN
e-mail: cjca@kth.se, web page: http://www.eco2vehicledesign.kth.se

[†]Technical Integration Engineer - Body Structure and Closures
Noise & Vibration Center
Saab Automobile AB
A2-1 TRV-05
SE-461 80, TROLLHÄTTAN, SWEDEN

ABSTRACT: *This paper deals with the design and weight optimization of a multi-functional vehicle body panel in an automotive context. An existing vehicle design has provided functional design requirements regarding static, dynamic, and acoustic behaviour of the components of a car roof. A novel, multifunctional panel is proposed which integrates the component requirements present in a traditional roof system within a single module. The acoustic properties of two configurations of the novel panel are examined using numerical methods including advanced poro-elastic modelling tools compatible with Nastran, and compared with numerical results of a finite element model of the existing construction.*

KEY WORDS: Sandwich Structures, Acoustic Modelling, Design Optimization.

INTRODUCTION

Common to all vehicles which transport either people or goods, is the need for certain functionality, such as protection and comfort, usually provided by a vehicle compartment, with different requirements depending on the vehicle application. For a passenger carrying vehicle, the compartment in general consists of the following components: body structure, acoustic treatments, and interior trim. Traditionally, these components have been designed, produced and assembled separately, each fulfilling different aspects of the protective functions, almost without exception with considerable weight penalty and often times with poor manufacturing efficiency and ergonomics during assembly.

To alleviate this, an approach based on simultaneous consideration of several such functions has been investigated. The main objective was to explore the potential benefits that may

be realized in a multi-functional, integrated multi-layered sandwich design. In this study, the performance in terms of noise, vibration, and harshness (NVH) characteristics and structural requirements of a proposed multi-functional component has been examined in an automotive context.

The vehicle of study in this case was a Saab 9-3 SportCombi. In selecting a panel for the study several areas of the vehicle were considered. The roof panel was chosen because it was of relatively simple geometry and relatively platform independent. Other panels such as the hood, doors and floor panel were considered, but deemed too constrained by regulatory legislation [1, 2] and too geometrically complex for an initial study. The roof structure is also subject to legislation however to a lesser extent [3].

In the frequency range below 500Hz, the primary source of interior noise is structure borne vibration from sources such as the power train or suspension system. Booming noise is the name given to the acoustic resonances within a vehicle's passenger cavity, usually under the frequency of 250 Hz [4]. The air cavity within the passenger compartment of a typical European station waggon will have a first acoustic mode in the region of 65-75Hz [5]. Even very small levels of vibration across large panel areas (such as the roof) can cause significant increases in sound pressure inside a vehicle interior [6] and potentially excite the cavities resonant modes of acoustic vibration. This is a major cause of discomfort for the passengers and for this reason, the roof is an acoustically relevant panel for study.

While a certain amount of local damping can be obtained by carefully designing joints within the structure [7], the traditional method of controlling structural borne vibration is with damping treatments in the form of visco-elastic material layers [8] . These damping treatments vary in form (free layer, constrained layer, bake-on,etc) and effectiveness, and a great deal of experimentation is usually involved in deciding the location and thickness of the damping layers [9, 10, 11].

In higher frequency ranges, air borne sound is prevalent, and sound management within the passenger compartment can be controlled via absorption [12]. This can be accomplished with absorbent insulation, interior trim components, seats, and floor matting [5]. Within the roof structure of a conventionally designed vehicle, the headliner and absorbent insulation coupled with the air gap between the headliner and the outer sheet metal are key components in minimizing unwanted external air borne sound from entering the vehicle.

In the current paper, which is an extension of work originally presented at ICSS-8 [13], a design concept is discussed wherein the components shown in Figure 1 are replaced with a multi-layer sandwich construction. By integrating the functionalities of structural components, acoustic treatments, and trim components into a single module which can offer mass savings, potential for acoustic improvements, and reduced assembly line time and effort, a novel method of addressing the requirements of a passenger enclosure were addressed. Two configurations were developed, one with a perforated inner face sheet and one without, which represented slightly different methods of dealing with acoustic fluid-structure interaction. Both configu-

rations were mass optimized according to current design requirements. Non–linear buckling analysis was performed to evaluate transverse load capacity. Finally, the NVH characteristics of the two configurations are evaluated numerically and compared with the conventional construction. Results of the optimization, buckling analysis, and acoustic analysis are given as well as a discussion of their interpretation.

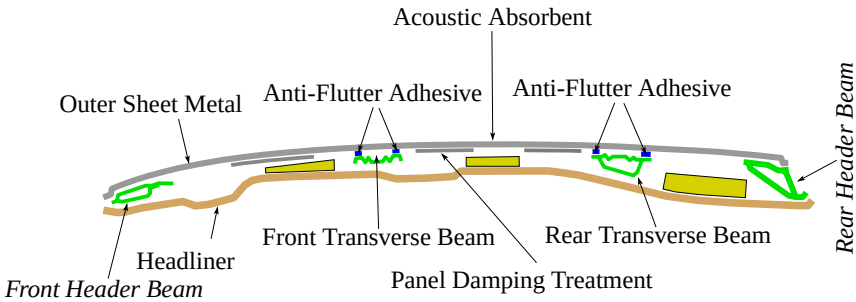

Figure 1: A Schematic cross-section of a conventional roof construction. Components in italics are not altered or replaced in the new concept.

METHOD

Engineering documentation provided by Saab Automobile AB (SAAB) was used together with static and dynamic finite element analysis of a the existing construction in order to establish the current state of the art. NXNastran 6.0 was used for static displacement analysis and modal analysis. Abaqus 6.7EF was used for non–linear buckling analysis.

A novel design was suggested and two configurations of the new panel were weight optimized against a set of static and dynamic constraints.

Non-linear buckling analysis of the optimized panels was performed to asses their in-plane loading capability in comparison to the existing construction.

NVH analysis was performed using the previously defined structural models and a vehicle fluid cavity, i.e. the air within the passenger compartment. Frequency response analysis including coupled fluid-structure effects was the method chosen. A model corresponding to the existing construction including the effects of the headliner trim was used to establish baseline behaviour. A second model corresponding to the proposed novel sandwich construction with integrated acoustic trim was created including new capabilities of modelling fluid-structure interactions in low-density poro-elastic foam materials. The acoustic performance of both the

baseline and concept configurations was assessed by exciting a point within fluid the cavity with an acoustic load and calculating the average sound pressure in the entire cavity.

BASELINE CONFIGURATION

Structural Modelling

A full vehicle model of the welded steel body and framework,often referred to as body in white (BIW), was provided by SAAB. As part of a testing program, SAAB also provided a complete roof assembly which had been removed from a production vehicle. The full vehicle FE model was reduced to match the provided roof structure as closely as possible . Figure 2 shows a the roof as removed from the vehicle and the FE model geometry. Note that in Figure 2 glass windows from the production vehicle have been replaced by medium density fibreboard (MDF) panels for acoustic testing purposes.

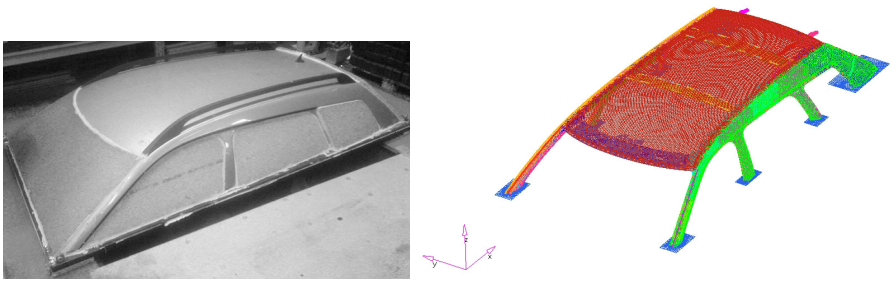

Figure 2: Roof structure removed from car and FE model.

The baseline configuration consists of short sections of the A, B, C, and D pillars, as well as longitudinal and lateral roof beams. The model used a combination of shell, solid, and rigid elements to represent various components such as sheet metal, adhesives, and spot welds.

Structural Target Setting

Static and dynamic stiffness requirements for body panels and the complete body in white were defined in the provided engineering documentation. Two requirements most relevant for the roof panel dictated static deflection under a prescribed load and minimum frequency for the first eigenmode of the panel.

Structural elements of the roof structure were not defined on an individual basis but assessed globally in the complete body in white. Further examination of the structural components in the roof assembly, in this case the lateral roof beams, was deemed necessary to further develop the

structural requirements for the new design.

Buckling analysis was considered a suitable method to evaluate the response of the roof beams located approximately between the B and C pillars in lateral loading. The front beam consists of a single pressed sheet metal component spot welded at each end to the longitudinal rails. A connection to the roof sheet metal is achieved using an elastic adhesive. The rear beam consists of two stamped steel components spot welded together forming a closed profile. Again, spot welds connect the beam to the longitudinal rails and a connection to the outer sheet metal is achieved by elastic adhesive. Both beams were analyzed using the modified Riks method in Abaqus.

The modified Riks method implemented in Abaqus standard is an incremental method of solving non-linear static problems such as buckling with snap through behaviour [14, 15]. By using a load proportionality factor and simultaneously varying the load and displacement, and calculating an equilibrium solution, the algorithm is capable of following the unstable collapse of a structure based on the assumptions that the response is smooth and no sudden bifurcations exist [16]. This seemed an appropriate method for the buckling analysis due to the nature of the problem and the geometry of the beam; slightly curved, thus having an initial instability.

As the rear beam is a closed profile rather than a pressed sheet it withstood a significantly higher buckling load and was deemed the more appropriate reference component.

Buckling analysis of the rear beam was performed in the following manner. The lower edge of one end of the beam was constrained in the translational degrees of freedom (DOF) but allowed to rotate. On the opposing end of the beam, the global x and z translational degrees of freedom were restricted, and a unit load in the global y direction was applied. For clarification, see Figure 3.

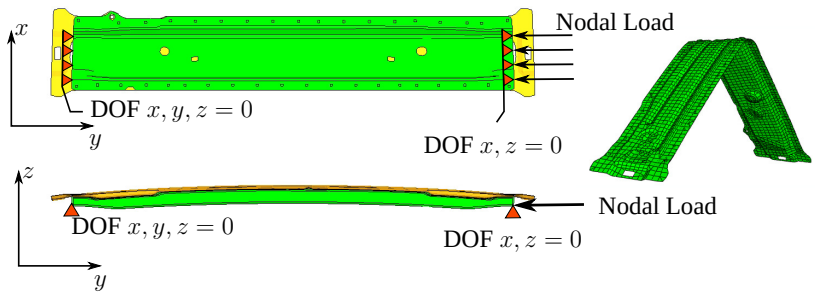

Figure 3: Rear beam boundary conditions and snap through buckling

To enable the large deformations present in the buckling analysis, plasticity was introduced into the model. Elastic, perfectly plastic material behaviour was modelled in Abaqus by spec-

ifying the yield stress, above which no further accumulation of stress occurs for plastic strains [16, 17].

A global y displacement of 200 mm for the end of the beam to which the load was applied was used as a parameter to stop the iterations during the modified Riks analysis. Within this distance, a maximum value for the load proportionality factor was reached, and snap-through buckling of the beam achieved (see Figure 3). By multiplying the maximum value of the load proportionality factor with the applied load for the buckling analysis, a value of the critical buckling load of the beam was obtained.

Modelling of Headliner Trim

In coupled fluid-structure analysis of the full vehicle, industrial practise is to ignore the acoustic effects of the inner headliner. The mass contribution of the inner roof trim may possibly be accounted for by adding a distributed non–structural mass to the interior of the roof sheet metal, or it may be ignored completely. While the headliner does have sound absorption capabilities due to the integration of open celled foam, at frequencies below several hundred hertz the thickness of the foam provides little contribution in relation to the other interior trim, such as the seats or carpet. While some limited work has been done in analyzing the effects of the roof cavity-headliner interaction [18] its effect is not well understood and seldom modelled numerically. The majority of information available regarding the acoustic or structural properties of headliners comes from the headliner manufacturers themselves [19, 20]. A method for numerically analyzing the acoustic properties of the acoustic trim would be an interesting step towards an independent in-situ design methodology and so was developed as part of the work in this paper.

The headliner studied was a sandwich construction consisting of two stiff fibre reinforced membranes separated by a foam core. On the interior side of the sandwich a second layer of relatively soft open–celled foam and a final layer of perforated fabric were used to provide sound absorption and an aesthetically appealing surface. Materials such as glass fibre reinforced plastics and polyurethane foam are often used in headliner applications [19, 20]. As uncertainties in the exact material composition existed, experimental testing was performed to obtain actual mechanical properties. Figure 4 shows a cross-section of the headliner in question.

A square approximately 35cm by 35cm was removed from the centre section of the headliner where the thickness was determined to be most uniform. The upper and lower membrane were peeled from the structural foam core, and the soft inner foam layer was peeled from the inner membrane. Each layer was trimmed to a square 25cm x25cm. The structural foam, assumed to be urethane, was weighed and its density calculated assuming a uniform thickness of 6.0 mm.

Tensile testing was performed according to ASTM standards [21]. This test method was used because the inner and outer membranes were of a glass fibre reinforced construction. Tabs for clamping were not considered necessary as the aim of the testing was to gain basic stiffness

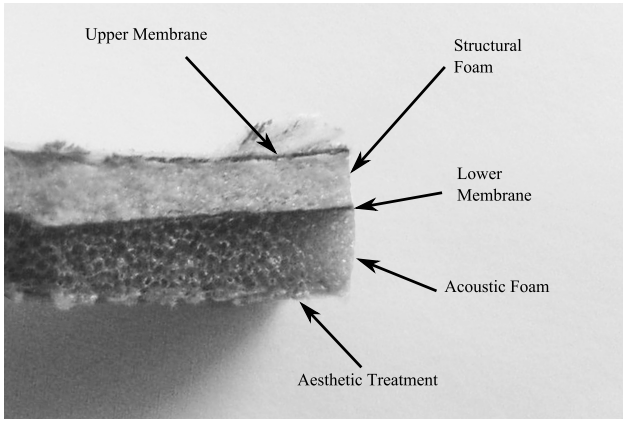

Figure 4: Cross-section of headliner construction

information not ultimate strength. The same testing method was used for testing the foam samples. While the choice of this test method for the foam samples was not optimal, it was deemed accurate enough to gain an estimate of the foams properties.

Ten samples measuring 25mm by 250mm were cut from the outer membrane, urethane foam, and inner membrane respectively. Samples were placed in pneumatic clamps fitted to an Instron screw driven Universal Testing Machine. An extensometer and a 30kN load cell were used to record the load vs displacement behaviour of the samples. The extensometer was attached to the sample using rubber bands. A picture of the sample in the test rig can be seen in Figure 5. Displacement control was used to regulate the rate of loading of the specimens.

Stress vs strain plots were obtained by post–processing the test results using Matlab™. Within the initial elastic region of the deformation, a first order polynomial curve was fitted to the data to achieve a value for the Young's modulus. This was repeated for each of the test specimens, and average values for each layer were calculated. Tensile Young's moduli of 9.1 GPa for the outer membrane and 4.8 GPa for the inner membrane were obtained. A tensile modulus of 8.8 MPa was obtained for the urethane foam.

For a glass fibre reinforced phenolic composite, values of Young's modulus in the range 4.5 - 7.5 GPa, depending upon whether the fibres are continuous or chopped, can be found within the literature [22]. This agrees well with test data for the inner and outer membranes, however it implies that another matrix material or some additional form of reinforcement is likely used in the outer membrane.

A density of 55.7 kg/m^3 was obtained for the urethane foam. According to [23] the relationship between the polymeric solid and its corresponding open–celled foam can be described as in Equation (1).

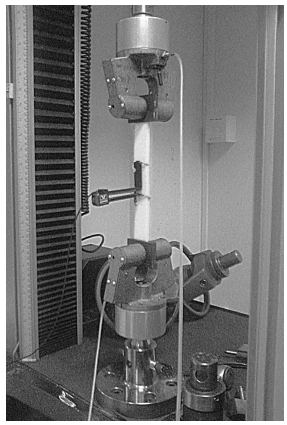

Figure 5: Tensile testing of headliner components

$$\frac{E_{foam}}{E_{solid}} \approx \left(\frac{\rho^{foam}}{\rho^{solid}}\right)^2 \tag{1}$$

Using the relationship in Equation (1) for the density calculated from the sample and using properties for solid polyurethane found in [23], a Young's modulus for the foam of 3.45 MPa was obtained. A compressive modulus of 10 MPa was listed in [22] for a polyurethane foam of slightly lower density (30kg/m^3). This data would seem to indicate a somewhat exaggerated estimate of the urethane foams properties achieved by tensile testing or perhaps a slightly different chemical makeup of the structural foam.

In the vehicle, the headliner effectively separates two fluid cavities, the fluid within the passenger compartment and the fluid between the headliner and the outer sheet metal. In order to achieve the physical distance between the two cavities, and to avoid mesh geometry and coupling difficulties between the fluid and the headliner, it was necessary to model the headliner using solid elements. In reality, the thickness of the headliner varies somewhat across the panel, due to the manufacturing process which often involves pressing [19], however a uniform thickness model was considered sufficient.

Accurate modelling of each individual layer of the headliner as shown in Figure 4 using only solid elements would be computationally quite expensive due to the small thicknesses and necessity for a great number of elements. Hybrid solid-shell sandwich configurations were also problematic due to the restrictions of the fluid-structure coupling capabilities of Nastran.

A modelling approach which could eliminate the requirement for excessive numbers of elements and which was more suitable to an industrial environment was desired. This was achieved

by modelling the headliner with equivalent homogeneous isotropic properties based on the mechanical properties measured and basic sandwich theory.

The upper three layers within the headliner make up a classical sandwich structure with dissimilar face sheets. The stiffness contribution of the aesthetic fabric treatment and the soft, porous acoustic foam to the overall stiffness of the headliner can be ignored.

Flexural rigidity for a unit width sandwich beam of arbitrary cross section with dissimilar face sheets can be expressed in the following manner [24]:

$$D = \int Ez^2 dz = \frac{E_1 t_1^3}{12} + \frac{E_2 t_2^3}{12} + \frac{E_c t_c^3}{12} + E_1 t_1 (d-e)^2 + E_2 t_2 e^2 + E_c t_c \left(\frac{t_c + t_2}{2} - e \right)^2 \quad (2)$$

Where:

$$e = \frac{E_1 t_1 d}{E_1 t_1 + E_2 t_2}$$

$$d - e = \frac{E_2 t_2 d}{E_1 t_1 + E_2 t_2}$$

$$d = \frac{t_1}{2} + t_c + \frac{t_2}{2}$$

The variable t denotes thickness, and E the Young's modulus for each respective layer. Subscripts 1 and 2 denote the upper and lower face sheets. Subscript c denotes the core material. In this case, the face materials are the two fibre reinforced membranes and the core the urethane foam layer. Lower case z denotes the vertical coordinate of the sandwich cross-section where $z = 0$ is the neutral axis of the sandwich structure.

A number of square samples were cut from the headliner and the thickness for each of the layers were measured. Thicknesses of the membranes, inner foam layer, and porous fabric layer were constant. The thickness of the structural foam varied from 1.5 mm to 6.0 mm, however based on samples taken and an estimate of compressed to non-compressed area, a nominal thickness of 4.0 mm was used in the FE model. The inner foam/fabric layer was constant at 2.0 mm.

Two layers of hexagonal solid (brick) elements were used to construct the headliner model following the geometry of the headliner's inner surface. The total thickness for the entire headliner in the model was 6.0 mm. Holes for attachment of lighting, etc., were ignored.

Using values of flexural rigidity calculated for an estimated core thickness of 4.0 mm and the measured stiffness for each of the various layers together with the mesh thickness of 6.0 mm, an equivalent value of Young's modulus, E_{equiv} , for the solid can be obtained as follows:

$$E_{equiv} = \frac{D}{\int z^2 dz} = \frac{D}{\frac{(6.0)^3}{3}} = 622.0[MPa] \tag{3}$$

Equivalent density was calculated by using the actual mass of the headliner and the volume of the headliner model according to:

$$\rho_{equiv} = \frac{M_{actual}}{V_{model}} \tag{4}$$

In the vehicle, the headliner was equipped with wiring and lighting systems. This mass was accounted for within the equivalent density calculation. The local stiffness effects of these components were ignored.

The headliner was attached to the structural model with rigid body elements at the actual attachment points. Nodes along the bottom front and rear edges were locked in translational degrees of freedom to approximate in vehicle conditions.

Acoustic Cavity Modelling

The internal geometry of the BIW was used to create air cavities for the two different analysis cases. For the conventional construction, the air cavity of the enclosed passenger compartment was split into two fluid volumes; fluid within the cab but below the headliner, and fluid between the headliner and the outer sheet metal of the roof. The two fluid cavities are connected by air channels within the A, B, C,and D pillars. These channels provide a fluid coupling between the cavities and the headliner provides a fluid–structure interface. To account for the acoustic absorption of the headliner, an acoustic impedance was applied to the cavity face in contact with the interior side of the headliner. Validation of the entire model including the headliner and split cavity was performed using acoustic and vibro-mechanical testing at the Markus Wallenberg Laboratory for sound and vibration research at KTH. Complete results are not included here, however the results of testing indicated that the modelling method agreed very well with experimental results up to 500 Hz [25].

For the case of the sandwich panels, a single cavity was used based on the same external geometry of the BIW and the underside of the sandwich panel. The same cavity was used for the evaluation of both sandwich panel configurations.

The cavity for the conventional configuration as well as the sandwich configuration were essentially identical in outer geometry and total volume. The cavities were mesh incompatible (i.e. no coincident nodes or elements) with the structural mesh geometry and consisted of approximately 1.5 million CTETRA elements each. Typical properties for air were used for describing the fluid cavities. Figure 6 shows a section view of the two models used for acoustic calculations.

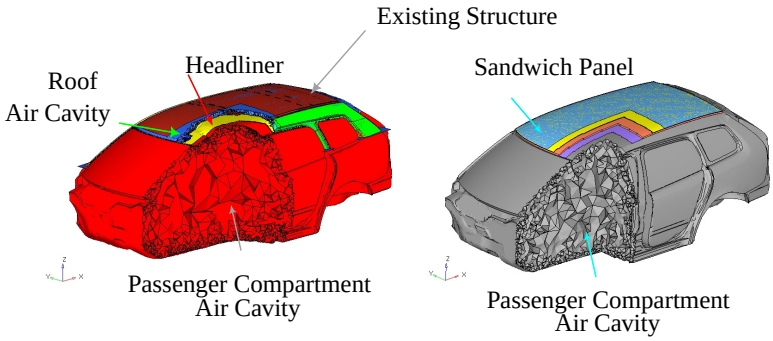

Figure 6: Partial section view of the two structural–acoustic models

Acoustic Target Setting

Acoustic targets for the new concept were defined using the FE model of the baseline structure.

Purely acoustic loading of the structure was achieved by applying an acoustic pressure to a single node within the vehicles passenger cavity. The node was located approximately at the drivers head and excited over the frequency range of 100-500 Hz in 2.5 Hz steps. The average acoustic pressure within the passenger cavity at each frequency was calculated using 270 nodes randomly distributed throughout the passenger cavity for the conventional configuration.

While this load cases was rather simplistic, it was deemed suitable for a preliminary NVH assessment.

MODELLING OF THE NEW PANEL CONCEPT

Both configurations of the proposed concept consisted of four components; external face sheets of isotropic material, a structural foam layer of typical polymeric sandwich core foam, and a single layer of lightweight, open–celled acoustic foam (see Figure 7). While structural polymer foam does offer a certain amount of damping [26], these properties were ignored within the model, as the damping treatments in the conventional model were also ignored.

In one panel configuration, the interior face sheet was perforated to allow fluid interaction between the passenger cavity and the acoustic foam, thus providing sound absorption in the interior of the panel. Geometry of the perforations is shown in Figure 7.

The non-perforated face sheets were modelled using aluminium because it is a lighter alternative to steel and is considered as a suitable material for mass production in the automotive industry [27]. For the structural optimization, both foam components were modelled as homogeneous elastic solids. Properties of a typical closed cell polymer foam sandwich core material were used for the structural foam component in the model. The acoustic foam modelled was

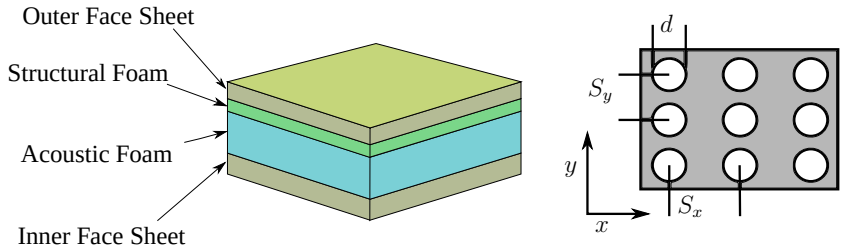

Figure 7: The four layer sandwich structure and perforation geometry

considerably softer than the other components. Material properties of the various layers as used in numerical analysis can be seen in Table 1.

Perforations on the interior face sheet are advantageous from an acoustic perspective because a proportion of incident sound waves pass into the structure and are absorbed rather than reflected. By allowing the air to flow within the open celled acoustic foam, additional structural and acoustic damping can be obtained. This phenomena is explained in detail in [28, 29]. As the degree of perforation in the face sheet is increased, so is the level of fluid-structure interaction between the passenger compartment fluid cavity and the absorbent foam (see Figure 8), however the structural capability of the face sheet is obviously reduced, a compromise which needs to be monitored closely.

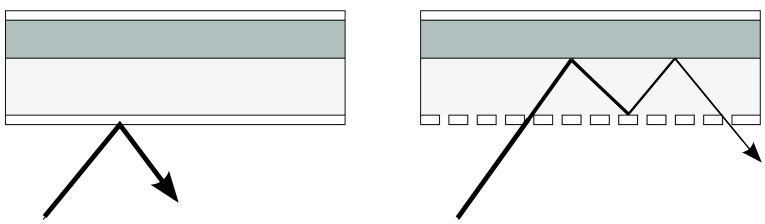

Figure 8: Incident sound wave behaviour for non-perforated and perforated face sheets

For the non-perforated sandwich panel, all four layers were considered isotropic and homogeneous.

For the perforated inner panel, modelling of individual perforations of such small geometry would create an extremely large number of elements in the model and make later acoustic analysis extremely difficult due to structural–acoustic coupling. Instead, a method of modelling the inner face sheet using a homogeneous mesh with perforation-equivalent properties was desired.

For a panel perforated with circular holes in a rectangular pattern as in Figure 7, the relative density ρ^* , based on the pre-drilled panel volume, can simply be calculated using the materials bulk density ρ and the hole pattern geometry. This relation is shown in Equation 5:

	Outer Face Sheet	Structural Foam	Acoustic Foam	Inner Face Sheet
Material	Aluminium	Closed Cell Foam	Open Cell Foam	Aluminium
E (MPa)	70 000	135	0.10	70 000 [46 460]
G (MPa)	26 000	35.0	–	26000 [–]
ρ (kg/m^3)	2710	100	30	2710 [2170]
ν	0.3	0.4	0.1	0.3 [0.27]

Table 1: Material properties in FE model for sandwich panels. In cases where properties differ, perforated values are shown inside square brackets

$$\rho^* = \rho \left(1 - \left[\frac{\pi}{4}\left(1 - \frac{S_x - d}{S_x}\right)\left(1 - \frac{S_y - d}{S_y}\right)\right]\right) \tag{5}$$

For a thin plate ($t \ll d$) with holes in a rectangular pattern ($S_x = S_y$) the literature [30, 31] provides a relationship between the bending stiffness D of a perforated and non–perforated plate as follows:

$$\frac{D^*}{D} = \left\{1 - \frac{\pi}{4}\left(1 - \frac{S_x - d}{S_x}\right)^2\right\}^{(2S_x - d)/0.8S_x} \tag{6}$$

Where D is simply:

$$D = \frac{E * t^2}{12(1 - \nu^2)} \tag{7}$$

Assuming then that the effect of the change in Poison's ratio (ν) is negligible, (in addition to the plate being very thin, according to the literature, for the hole pattern used there is only a 0.1% reduction in Poisson's ratio [32]) the same relationship can be used to describe the relative Young's modulus E^* of the perforated plate based on hole geometry as shown in Equation (8) :

$$E^* = E\left\{1 - \frac{\pi}{4}\left(1 - \frac{S_x - d}{S_x}\right)^2\right\}^{(2S_x - d)/0.8S_x} \tag{8}$$

In this study the values $d = 2.0$ mm and $S_x = S_y = 4.0$ mm were used for the perforated inner face sheet.

For the analysis performed, the simplifications caused by using equivalent isotropic materials instead of modelling a perforated plate caused little loss in accuracy in return for exceptional decreases in modelling complexity and calculation time. It should be noted that effects of

stress concentrations at the perforations were not accounted for, however the effect of such concentrations on the analysis performed is expected to be insignificant.

Mesh geometry for the outer sheet metal in the conventional roof was used to construct an FE model of a sandwich panel. Each panel was modelled using approx. 235000 three dimensional CHEXA [33] elements. Two different sets of boundary conditions were used for the panel analysis during optimization. For the static displacement analysis, translational degrees of freedom x, y, z for all nodes along the bottom edge of the panel were constrained. For the modal analysis, it was necessary to constrain additional nodes along the sides due to the soft acoustic foam layer. Translational degrees of freedom x, y, z of all nodes along the side edges and rear edge were constrained in addition to the lower front edge. A comparison of modal behaviour with the existing structure showed good agreement using these boundary conditions. See Figure 9 for clarification.

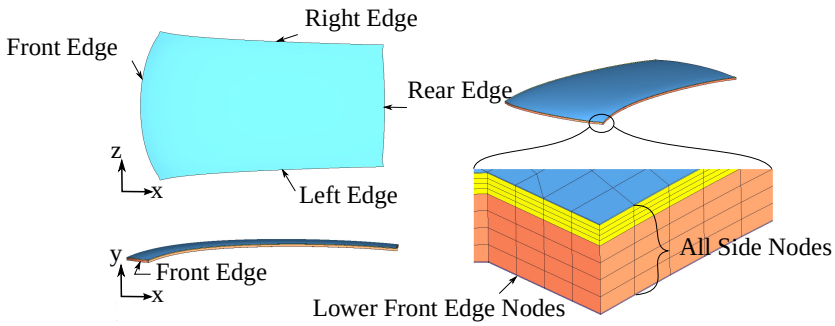

Figure 9: Diagram of complete sandwich panel

STRUCTURAL OPTIMIZATION

Both panel configurations were weight optimized using the method of moving asymptotes[34] implemented in the optimization software Xopt developed by Alfgam Optimering AB[1]. Geometry manipulation was achieved by the use of a python script to alter the nodal coordinates of elements.

Design constraints were placed on the static displacement under load as well as the frequency of the first mode of the panel. Thickness of the internal face sheet, external face sheet, and structural foam layer were chosen as design variables. Changes in thickness were evenly distributed through each of the element layers in a given material in an effort to maintain an even FE mesh. The lower limit for each layers thickness was defined so that the aspect ratio of 3D elements would not exceed 50. At the outset of optimization, this limit was considered sufficiently thin as to be far below any probable solution.

[1]www.alfgam.se

	Outer Face Sheet	Structural Foam	Acoustic Foam	Inner Face Sheet
Min thickness (mm)	0.2000	0.5000	15	0.2000
Max thickness (mm)	12.0000	20.0000	15	7.0000
Final thickness (mm)	0.2000	4.6004[5.088]	15	0.2000

Table 2: Optimization variables for sandwich panels. In cases where values differ, perforated values are shown inside square brackets

	Perforated Panel	Non-Perforated Panel
Optimized Mass(% of Conventional)	17.643	18.215
Active Constraint	Static displacement	Static displacement

Table 3: Optimization results for perforated and non-perforated panels

Table 2 shows the final thickness of the optimized panel. Inner and outer face sheets for both panels were reduced to the minimum allowable thickness. Thickness of the structural foam varied approximately 10% between the perforated and non–perforated panel. Acoustic foam thickness was held constant at 15 mm.

Table 3 shows further results of the optimization. Final mass of the panels varied by less than 1% in comparison to the conventional construction. Results show that static displacement rather than natural frequency was the limiting factor for the optimization of the panels. Convergence to a stable solution was achieved within 10 iterations. Both panels fulfilled displacement constraints and exceeded frequency constraints by approximately 15%.

PANEL BUCKLING ANALYSIS

After the weight optimization was completed, the panel's resistance to buckling during in-plane loading was examined using the modified Riks method in Abaqus.

Loading and boundary conditions for the panel were as follows.

Nodes along the bottom edge of one side of the panel were clamped by restricting all translational degrees of freedom. Nodes along the bottom edge of the opposite side were restricted from moving in the x and z directions, as was the case for the beam. A unit nodal load was applied in the y direction to all nodes which were locked in the x and z directions. As was the case for the beam buckling analysis, plasticity was also introduced for the materials in the sandwich panels. Typical yield stress values for aluminium and structural foam were used. No plasticity was implemented for the acoustic foam as its contribution to stiffness was minimal.

Two stop criteria for the panel buckling analysis were used. The same maximum displacement criterion was applied to the panel as to the beams. Additionally, a maximum load proportionality factor yielding the same maximum buckling load as in the beam analysis was used.

Analysis of both panels resulted in the maximum load proportionality factor being exceeded before the maximum deformation occurred, i.e. both panels were capable of supporting the maximum buckling load without snap-through buckling.

ACOUSTIC EVALUATION

Finite element analysis was used to compare the acoustic properties of the two optimized panels to each other, and to the current state of the art construction. As previously mentioned, two different models were necessary in order to carry out this analysis; one model for the current passenger compartment including the headliner and one model for the sandwich panels with integrated acoustic treatments.

Setup of Analysis

The sandwich panel model consisted of the sandwich panel geometry and the passenger fluid cavity. For the case of the conventional construction, the partial vehicle model was included in addition to the roof and passenger fluid cavities. For clarification, refer to Figure 6. Boundary conditions were placed on the structural components only for acoustic analysis. For the sandwich panels an attempt to emulate in–service conditions was made by restricting all nodes along both the sides and the rear edge of the panel in x, y, z direction in addition to the nodes along the front lower edge of the panel. For the conventional construction, the bottom of the pillars were constrained in x, y, z.

The acoustic volume was coupled to the structure via automated algorithms in Nastran [35]. For a standard fluid–structure coupling, the translational degrees of freedom in a solid element are linked to the first translational degree of freedom in a fluid element which is interpreted as pressure [36]. These standard fluid structure couplings were used for the non-perforated sandwich panel, and the standard construction in analysis.

For the case of the perforated sandwich panel, the software CDH\EXEL by CDH AG[2] was used in combination with NXNastran 6.0. CDH\EXEL is a proprietary software which augments the standard functionality of Nastran in coupled fluid–structure analysis by adding a fourth degree of freedom to solid elements matrices representing open cell porous materials. Frequency dependant material properties can be defined in a way not previously possible with Nastran. The augmented structural elements matrices are used to calculate the effects of fluid pressure within a porous media. As part of the CDH\EXEL suite, CDH\CONNECT was used to automatically produce the coupling equations (Multi–Point Constraints(MPC)) between the fluid cavity and the porous media as well as the porous media to the conventional solid elements. For a given node in the porous solid, the resulting DOF matrix will appear as in Equation (9)

[2]http://www.cdh-ag.com/de/exel.html

$$\left[\begin{array}{c|c} {}^{Nastran}_{solid}\mathbf{D}_{ij}(\omega) + {}^{Exel}_{solid}\mathbf{D}_{ij}(\omega) & symm \\ \hline {}^{Exel}_{coupling}\mathbf{D}_{4j}(\omega) & {}^{Exel}_{fluid}\mathbf{D}_{44}(\omega) \end{array}\right]^{inode}_{jnode} \tag{9}$$

The acoustic foam and the perforated face sheet in the perforated sandwich panel are modelled using the porous, elastic solid model. Properties such as frequency dependancy and flow resistivity were taken from laboratory testing performed at KTH.

Results of Acoustic Analysis

Frequency response analysis for the sandwich panel configurations was performed in the same manor as for the conventional roof. For these calculations, acoustic response within the cavity was calculated using the sound pressure at approximately 370 randomly situated points within the cavity. Results for both conventional and sandwich configurations can be seen in Figure 10.

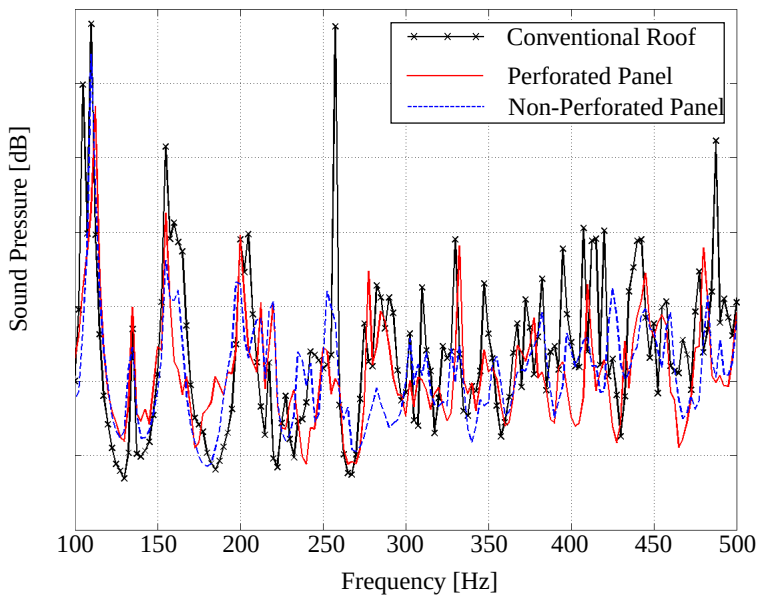

Figure 10: Average sound pressure in cavity vs excitation frequency (Y-axis 5 dB steps)

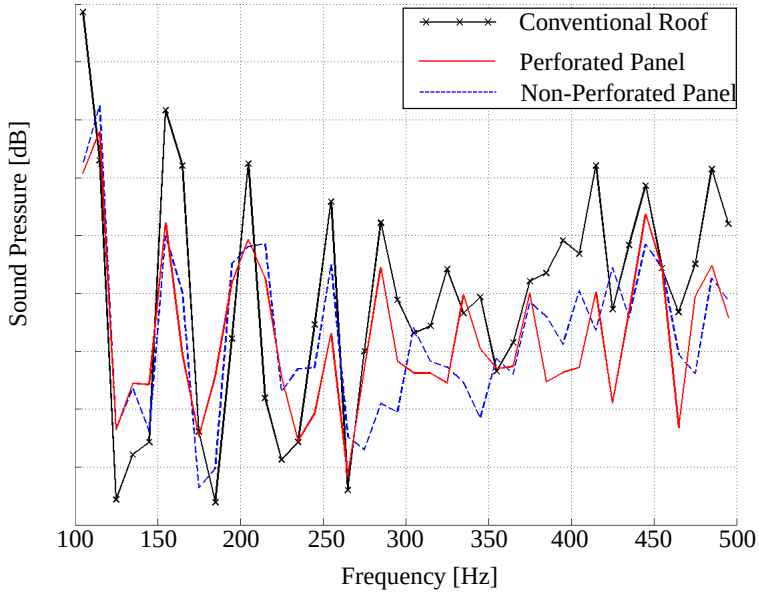

Figure 11: Average sound pressure in cavity vs excitation frequency (Y-axis 5 dB steps)

Looking at the results in Figure 10 it can be seen that the general behaviour of all three configurations is quite similar. This result is, from an acoustic standpoint, very significant; despite the fact that mass has been drastically reduced in the system, no noticeable degradation of the acoustic environment has taken place.

More detailed inspection of Figure 10 reveals that while the step in excitation frequency is relatively small (2.5 Hz) at certain points, the response levels off somewhat drastically, indicating that some resonance peaks have been slightly missed. While this is arguably a point for further investigation, it is unlikely that higher frequency resolution would yield a significant change in the overall response.

Figure 11 shows the same results as obtained in Figure 10, however levels have been averaged over 10 Hz intervals. Here, the differences between the conventional and sandwich configurations are much clearer. Figure 11 shows without doubt that no degradation of the acoustic performance has taken place in spite of the significant reduction of mass. It would also appear, that in the frequency range above 300Hz, the sandwich constructions in fact perform better overall than the conventional design. Differentiating between the perforated and non-perforated configuration is somewhat more difficult. At some frequencies the perforated panel

appears to perform better, and at others the non-perforated.

DISCUSSION

From a design perspective, it is interesting to note that during the optimization, the active constraint was that of static displacement and not dynamic stiffness. It is also interesting to note that the final thickness of the face sheets is very thin and would likely lead to handling problems in production. In this case, the thickness of the structural foam was an active variable. Based on these results, it would be interesting to further investigate the effects of altering the structural foam or face sheet material properties.

Buckling analysis of the optimized panels shows that despite a non-conventional sandwich construction, both sandwich panels are capable of supporting an equivalent buckling load compared to that of the transverse beams that the sandwich would be replacing. For this analysis, it has been assumed that transverse loading would be evenly spread across the entire length of the sandwich panel. While this may hold true for a number of load cases, it would seem a logical next step to investigate more localized loading behaviour.

One area of debate is that of the boundary conditions used in analysis of the sandwich panels. While a great deal of effort has been made in trying to model the two configurations as similar as possible, it is extremely difficult to apply exactly similar boundary conditions to two fundamentally different constructions. Due to the primitive stage of development of the concept it could not be included in the framework of the conventional roof and there was little other choice than to use the boundary conditions described. The effects of variations in the boundary conditions on the overall output of the work are considered to be minimal.

From an acoustic perspective, the results as presented in Figures 10 and 11, are very promising. A significant reduction in mass of the system has taken place with no degradation of the acoustic performance. Results would even seem to indicate a slight improvement in performance in certain frequency ranges.

Throughout the optimization the acoustic characteristics of the panel have remained static; a fixed acoustic foam thickness and fixed perforation pattern have been used. While it is difficult to differentiate the superiority of the perforated or non-perforated sandwich configurations, what can be said with certainty is that while the non-perforated concept represents a fixed minima in acoustic performance via absorbance, the perforated configuration shows promise in that it offers room for improvement. Results of the structural optimization indicate that the interior face sheet can afford a significant reduction in stiffness, and thus a significant increase in the degree of perforation. This would be advantageous from an acoustic perspective. The significant reduction in mass for the system also allows for a large design space regarding future optimization of the acoustic functionality while still reducing weight.

CONCLUSIONS

Two different configurations of sandwich panel have been proposed, and weight optimized against a set of structural requirements obtained from engineering documentation and analysis of an existing verified FE model. Each panel consists of four layers; two face sheets, one layer of acoustic foam, and one layer of structural foam. For one of the panels, the inner face sheet is perforated. The effect of the perforations on the weight optimization has very little effect on the outcome of the structural optimization, both panels varying only slightly in mass and thickness. After optimization, the panels were evaluated using non-linear buckling analysis to asses potential to support transverse loading. Finally, the acoustic properties of the panels are assessed over a range of frequencies and compared with the current state of the art.

The concept of a multifunctional body panel having structural and acoustic functionality has been explored, and results show promise. A reduction in mass of more than 80% compared to the conventional configuration was achieved for both sandwich configurations while still fulfilling static and dynamic stiffness constraints. Both sandwich panels are capable of sustaining a uniform transverse in–plane load equivalent to the maximum buckling load of the rear transverse beam of the conventional construction. Coupled fluid structure analysis shows that both sandwich configurations behave similarly to the conventional configuration and despite the vast reduction in mass, no acoustic degradation occurs and in fact a small improvement may have been achieved. Results of the optimization yield a broad design space for future structural and acoustic improvements regarding the materials and configuration of the structural components and the acoustic treatment.

ACKNOWLEDGEMENTS

This work was performed within the Centre for ECO^2 Vehicle Design with financial support from the Swedish Agency for Innovation Systems (VINNOVA), KTH, and Saab Automobile AB. The financial support is gratefully acknowledged.

Additionally, the generous provision of the CDH\EXEL software by CDH AG and the assistance of Mr. Mladen Chargin is hereby gratefully acknowledged.

REFERENCES

[1] National Highway Traffic Safety Administration, “Federal motor vehicle safety standard no. 208; occupant crash protection.”

[2] National Highway Traffic Safety Administration, “Federal motor vehicle safety standard no. 214; side impact protection.”

[3] National Highway Traffic Safety Administration, “Federal motor vehicle safety standard no. 216; roof crush resistance.”

[4] S.-H. Oh, H.-S. Kim, and Y. Park, "Active control of road booming noise in automotive interiors," *Journal of the Acoustical Society of America*, vol. 111, pp. 180–188, Jan 2002.

[5] M. Harrison, *Vehicle Refinement Controlling Noise and Vibration in Road Vehicles*. Elsevier Butterworth-Heinemann, 2004.

[6] R. F. Freymann, "Advanced numerical and experimental methods in the field of vehicle structural-acoustics," 2000. ISBN:3-89791-172-8.

[7] A. Kropp and F. Ihlenburg, "Influence of local damping on the acoustic design of passenger car bodies," *AutoTechnology*, vol. 4, pp. 60–63, Aug 2004.

[8] M. D. Rao, "Recent applications of viscoelastic damping for noise control in automobiles and commercial aeroplanes," *Journal of Sound and Vibration*, vol. 262, pp. 457–474, May 2003.

[9] S. Subramanian, R. Surampudi, K. Thomson, and S. Vallurupalli, "Optimization of damping treatments for structure borne noise reduction," *Sound and Vibration*, vol. 38, pp. 14–18, Sept 2004.

[10] S.M.Beane, M.M.Marchi, and D.S.Snyder, "Utilizing optimized panel damping treatments to improve powertrain induced nvh and sound quality," *Applied Acoustics*, vol. 45, no. 2, pp. 181–187, 1995.

[11] J.Bienert, "Optimisation of damping layers in car bodies," *Proceedings of the 2002 International Conference on Noise and Vibration Engineering, ISMA*, pp. 2005–2010, Sept 2002.

[12] X.Sagartzazu, L. Hervella-Nieto, and J. Pagalday, "Review in sound absorbing materials," *Archives of Computational Methods in Engineering*, vol. 15, pp. 311–342, 2008.

[13] C. J. Cameron, P. Wennhage, P. Göransson, and S. Rhamqvist, "Structural-acoustic design of a multi-functional body panel for automotive applications," in *8th INTERNATIONAL CONFERENCE ON SANDWICH STRUCTURES(ICSS8)* (A. J. Ferreira, ed.), vol. 2, pp. 896–907, 2008.

[14] E. Riks , "An incremental approach to the solution of snapping and buckling problems," *International Journal of Solids and Structures*, vol. 15, no. 7, pp. 529–551, 1979.

[15] Dassault Systèmes Simulia Corp., *Abaqus Theory Manual, Version 6.7 EF*, 2007.

[16] Dassault Systèmes Simulia Corp., *Abaqus Analysis Users Manual, Version 6.7 EF*, 2007.

[17] Dassault Systèmes Simulia Corp., *Abaqus Keywords Reference Manual, Version 6.7 EF*, 2007.

[18] H. G. Choi, S. W. Kang, S. H. Lee, and J. M. Lee, "A coupling analysis of interior noise of a vehicle with a roof-gap-trim effect," in *Proceedings of the 15 International Modal Analysis Converence-IMAC*, pp. 444–449, SEM, Bethel, CT, USA, February 1997.

[19] J. Stoll and D. G. Schlotterbeck, "Headliners and other interior trim parts made of thermoformable urethane foam core sandwiches," *SAE Technical Paper Series*, vol. 900827, 1990.

[20] E. Haque, "Designing strength, stiffness and acoustics in headliner substrate material," *Auto Technology*, vol. 5, pp. 42–45, 2006.

[21] ASTM, "Astm d3039/d3039m standard test method for tensile properties of polymer matrix composite materials," tech. rep., 2000.

[22] B.T.Åström, *Manufacturing of Polymer Composites*. Chapmann & Hall, 1997.

[23] L. J. Gibson and M. F. Ashby, *Cellular Solids: Structure and Properties-Second edition*. Cambridge University Press, 1997.

[24] D. Zenkert, *An Introduction to Sandwich Construction*. Engineering Materials Advisory Services Ltd., EMAS, Solihull, UK, 1995.

[25] C. J. Cameron, P. Wennhage, and P. Göransson, "Prediction and measurement of noise and vibration behavior of trimmed body components at mid-frequencies," *Submitted for publication to 'APPLIED ACOUSTICS', March 2009*.

[26] H.Kolsters and P.Wennhage, "Density and frequency dependence of loss factor of foam core materials," *Proceedings of the Fifth International Conference on Sandwich Constructions*, vol. 2, pp. 429–440, 2000.

[27] G.S.Cole and A.M.Sherman, "Lightweight materials for automotive applications," *Materials Characterization*, vol. 35, pp. 3–9, 1995.

[28] P. Göransson, "Tailored acoustic and vibrational damping in porous solids – engineering performance in aerospace applications," *Aerospace Science and Technology*, vol. 12, pp. 26–41, 2008.

[29] P. Göransson, "Acoustic and vibrational damping in porous solids," *Phil. Trans. R. Soc. A*, vol. 364, pp. 89–108, 2005.

[30] A.I.Soler and W.S.Hill, "Effective bending properties for stress analysis of rectangular tubesheets," *Transactions of the ASME: Journal of Engineering for Power*, pp. 365–370, July 1977.

[31] K.A.Burgemeister and C.H.Hansen, "Calculating resonance frequencies of perforated panels," *Journal of Sound and Vibration*, vol. 196, pp. 387–399, Oct 1996.

[32] M.Forskitt, J.R.Moon, and P.A.Brook, “Elastic properties of plates perforated by elliptical holes,” *Applied Mathematical Modelling*, vol. 15, pp. 182–190, April 1991.

[33] UGS Corporation, *NX Nastran Quick Reference Guide*, 2007.

[34] K. Svanberg, “The method of moving asymptotes-a new method for structural optimization,” *International Journal for Numerical Methods in Engineering*, vol. 24, pp. 359–373, Feb 1987.

[35] UGS Corporation, *NX Nastran Advanded Dynamic Analysis Users Guide*, 2007.

[36] UGS Corporation, *NX Nastran User Guide*, 2007.